WCAP-14191

SCALING ANALYSIS FOR AP600 PASSIVE

CONTAINMENT COOLING SYSTEM

October 1994

by

D. R. Spencer

WESTINGHOUSE ELECTRIC CORPORATION
Nuclear Technology Division
P. O. Box 355
Pittsburgh, Pennsylvania 15230-355

u:\1462w.non:1b-102694

AP600 DOCUMENT COVER SHEET

TDC: _____   IDS: I _____ S _____

Form 58202G(5/94)   AP600 CENTRAL FILE USE ONLY:

0058.FRM   RFS#: _____   RFS ITEM #: _____

AP600 DOCUMENT NO.	REVISION NO.		ASSIGNED TO
PCS-GSR-005	0	Page 1 of	

ALTERNATE DOCUMENT NUMBER: WCAP 14190 & 14191   WORK BREAKDOWN #: 2.2.6.6.2

DESIGN AGENT ORGANIZATION: WESTINGHOUSE

TITLE: Scaling Analysis for AP600 Passive Containment Cooling System

ATTACHMENTS: N/A

DCP #/REV. INCORPORATED IN THIS DOCUMENT REVISION: N/A

CALCULATION/ANALYSIS REFERENCE: 522

ELECTRONIC FILENAME	ELECTRONIC FILE FORMAT	ELECTRONIC FILE DESCRIPTION
U:\ap600\1462w.non U:\ap600\1462frm.non	WORDPERFECT 5.2 WINDOWS	DOCUMENT TEXT AND FIGURES

(C) WESTINGHOUSE ELECTRIC CORPORATION 1994

COMPLETE 1 IF WORK PERFORMED UNDER DESIGN CERTIFICATION OR COMPLETE 2 IF WORK PERFORMED UNDER FOAKE.

1 ☒ DOE DESIGN CERTIFICATION PROGRAM – GOVERNMENT LIMITED RIGHTS STATEMENT [See page 2]

Copyright statement: A license is reserved to the U.S. Government under contract DE-AC03-90SF18495.

☐ DOE CONTRACT DELIVERABLES (DELIVERED DATA)
Subject to specified exceptions, disclosure of this data is restricted until September 30, 1995 or Design Certification under DOE contract DE-AC03-90SF18495, whichever is later.
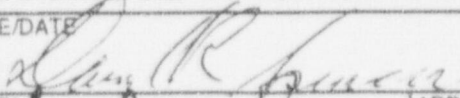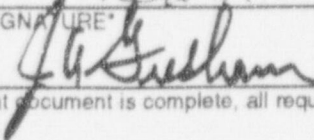
EPRI CONFIDENTIAL: NOTICE: 1☐ 2☐ 3☒ 4☐ 5☐ CATEGORY: A☒ B☐ C☐ D☐ E☐ F☐

2 ☐ ARC FOAKE PROGRAM – ARC LIMITED RIGHTS STATEMENT [See page 2]

Copyright statement: A license is reserved to the U.S. Government under contract DE-FC02-NE34267 and subcontract ARC-93-3-SC-001.

☐ ARC CONTRACT DELIVERABLES (CONTRACT DATA)
Subject to specified exceptions, disclosure of this data is restricted under ARC Subcontract ARC-93-3-SC-001.

ORIGINATOR	SIGNATURE/DATE	
D. R. Spencer	*[signature]*	10/27/94
AP600 RESPONSIBLE MANAGER	SIGNATURE	APPROVAL DATE
J. A. Gresham	*[signature]*	10/27/94

*Approval of the responsible manager signifies that document is complete, all required reviews are complete, electronic file is attached and document is released for use.

Form 58202G(5/94)

LIMITED RIGHTS STATEMENTS

DOE GOVERNMENT LIMITED RIGHTS STATEMENT

(A)   These data are submitted with limited rights under government contract No. DE-AC03-90SF18495. These data may be reproduced and used by the government with the express limitation that they will not, without written permission of the contractor, be used for purposes of manufacturer nor disclosed outside the government; except that the government may disclose these data outside the government for the following purposes, if any, provided that the government makes such disclosure subject to prohibition against further use and disclosure:

      (I)   This "Proprietary Data" may be disclosed for evaluation purposes under the restrictions above.

      (II)   The "Proprietary Data" may be disclosed to the Electric Power Research Institute (EPRI), electric utility representatives and their direct consultants, excluding direct commercial competitors, and the DOE National Laboratories under the prohibitions and restrictions above.

(B)   This notice shall be marked on any reproduction of these data, in whole or in part.

ARC LIMITED RIGHTS STATEMENT:

This proprietary data, furnished under Subcontract Number ARC-93-3-SC-001 with ARC may be duplicated and used by the government and ARC, subject to the limitations of Article H-17.F. of that subcontract, with the express limitations that the proprietary data may not be disclosed outside the government or ARC, or ARC's Class 1 & 3 members or EPRI or be used for purposes of manufacture without prior permission of the Subcontractor, except that further disclosure or use may be made solely for the following purposes:

This proprietary data may be disclosed to other than commercial competitors of Subcontractor for evaluation purposes of this subcontract under the restriction that the proprietary data be retained in confidence and not be further disclosed, and subject to the terms of a non-disclosure agreement between the Subcontractor and that organization, excluding DOE and its contractors.

DEFINITIONS

CONTRACT/DELIVERED DATA — Consists of documents (e.g. specifications. drawings, reports) which are generated under the DOE or ARC contracts which contain no background proprietary data.

EPRI CONFIDENTIALITY / OBLIGATION NOTICES

NOTICE 1: The data in this document is subject to no confidentiality obligations.

NOTICE 2: The data in this document is proprietary and confidential to Westinghouse Electric Corporation and/or its Contractors. It is forwarded to recipient under an obligation of Confidence and Trust for limited purposes only. Any use, disclosure to unauthorized persons, or copying of this document or parts thereof is prohibited except as agreed to in advance by the Electric Power Research Institute (EPRI) and Westinghouse Electric Corporation. Recipient of this data has a duty to inquire of EPRI and/or Westinghouse as to the uses of the information contained herein that are permitted.

NOTICE 3: The data in this document is proprietary and confidential to Westinghouse Electric Corporation and/or its Contractors. It is forwarded to recipient under an obligation of Confidence and Trust for use only in evaluation tasks specifically authorized by the Electric Power Research Institute (EPRI). Any use, disclosure to unauthorized persons, or copying this document or parts thereof is prohibited except as agreed to in advance by EPRI and Westinghouse Electric Corporation. Recipient of this data has a duty to inquire of EPRI and/or Westinghouse as to the uses of the information contained herein that are permitted. This document and any copies or excerpts thereof that may have been generated are to be returned to Westinghouse, directly or through EPRI, when requested to do so.

NOTICE 4: The data in this document is proprietary and confidential to Westinghouse Electric Corporation and/or its Contractors. It is being revealed in confidence and trust only to Employees of EPRI and to certain contractors of EPRI for limited evaluation tasks authorized by EPRI. Any use, disclosure to unauthorized persons, or copying of this document or parts thereof is prohibited. This Document and any copies or excerpts thereof that may have been generated are to be returned to Westinghouse, directly or through EPRI, when requested to do so.

NOTICE 5: The data in this document is proprietary and confidential to Westinghouse Electric Corporation and/or its Contractors. Access to this data is given in Confidence and Trust only at Westinghouse facilities for limited evaluation tasks assigned by EPRI. Any use, disclosure to unauthorized persons, or copying of this document or parts thereof is prohibited. Neither this document nor any excerpts therefrom are to be removed from Westinghouse facilities.

EPRI CONFIDENTIALITY / OBLIGATION CATEGORIES

CATEGORY "A" — (See Delivered Data) Consists of CONTRACTOR Foreground Data that is contained in an issued reported.

CATEGORY "B" — (See Delivered Data) Consists of CONTRACTOR Foreground Data that is not contained in an issued report, except for computer programs.

CATEGORY "C" — Consists of CONTRACTOR Background Data except for computer programs.

CATEGORY "D" — Consists of computer programs developed in the course of performing the Work.

CATEGORY "E" — Consists of computer programs developed prior to the Effective Date or after the Effective Date but outside the scope of the Work.

CATEGORY "F" — Consists of administrative plans and administrative reports.

AP600 DOCUMENT COVER SHEET

TDC: _____   IDS: I_____ S_____

Form 58202G(5/94)

AP600 CENTRAL FILE USE ONLY:

0058.FRM

RFS#: _____   RFS ITEM #: _____

AP600 DOCUMENT NO.	REVISION NO.		ASSIGNED TO
PCS-GSR-005	0	Page 1 of	

ALTERNATE DOCUMENT NUMBER: WCAP 14190 & 14191   WORK BREAKDOWN #: 2.2.6.6.2

DESIGN AGENT ORGANIZATION: WESTINGHOUSE

TITLE: Scaling Analysis for AP600 Passive Containment Cooling System

ATTACHMENTS: N/A

DCP #/REV. INCORPORATED IN THIS DOCUMENT REVISION: N/A

CALCULATION/ANALYSIS REFERENCE: 522

ELECTRONIC FILENAME	ELECTRONIC FILE FORMAT	ELECTRONIC FILE DESCRIPTION
U:\ap600\1462w.non U:\ap600\1462frm.non	WORDPERFECT 5.2 WINDOWS	DOCUMENT TEXT AND FIGURES

(C) WESTINGHOUSE ELECTRIC CORPORATION 1994

COMPLETE 1 IF WORK PERFORMED UNDER DESIGN CERTIFICATION OR COMPLETE 2 IF WORK PERFORMED UNDER FOAKE.

ORIGINATOR	SIGNATURE/DATE	
D. R. Spencer	*[signature]*	10/27/94
AP600 RESPONSIBLE MANAGER	SIGNATURE	APPROVAL DATE
J. A. Gresham	*[signature]*	10/27/94

*Approval of the responsible manager signifies that document is complete, all required reviews are complete, electronic file is attached and document is released for use.

LIMITED RIGHTS STATEMENTS

Form 58202G(5/94)

DOE GOVERNMENT LIMITED RIGHTS STATEMENT

(A)   These data are submitted with limited rights under government contract No. DE-AC03-90SF18495. These data may be reproduced and used by the government with the express limitation that they will not, without written permission of the contractor, be used for purposes of manufacture nor disclosed outside the government; except that the government may disclose these data outside the government for the following purposes, if any, provided that the government makes such disclosure subject to prohibition against further use and disclosure:
- (I)   This "Proprietary Data" may be disclosed for evaluation purposes under the restrictions above.
- (II)   The "Proprietary Data" may be disclosed to the Electric Power Research Institute (EPRI), electric utility representatives and their direct consultants, excluding direct commercial competitors, and the DOE National Laboratories under the prohibitions and restrictions above.

(B)   This notice shall be marked on any reproduction of these data, in whole or in part.

ARC LIMITED RIGHTS STATEMENT:

This proprietary data, furnished under Subcontract Number ARC-93-3-SC-001 with ARC may be duplicated and used by the government and ARC, subject to the limitations of Article H-17.F. of that subcontract, with the express limitations that the proprietary data may not be disclosed outside the government or ARC, or ARC's Class 1 & 3 members or EPRI or be used for purposes of manufacture without prior permission of the Subcontractor, except that further disclosure or use may be made solely for the following purposes:

This proprietary data may be disclosed to other than commercial competitors of Subcontractor for evaluation purposes of this subcontract under the restriction that the proprietary data be retained in confidence and not be further disclosed, and subject to the terms of a non-disclosure agreement between the Subcontractor and that organization, excluding DOE and its contractors.

DEFINITIONS

CONTRACT/DELIVERED DATA — Consists of documents (e.g. specifications, drawings, reports) which are generated under the DOE or ARC contracts which contain no background proprietary data.

EPRI CONFIDENTIALITY / OBLIGATION NOTICES

NOTICE 1: The data in this document is subject to no confidentiality obligations.

NOTICE 2: The data in this document is proprietary and confidential to Westinghouse Electric Corporation and/or its Contractors. It is forwarded to recipient under an obligation of Confidence and Trust for limited purposes only. Any use, disclosure to unauthorized persons, or copying of this document or parts thereof is prohibited except as agreed to in advance by the Electric Power Research Institute (EPRI) and Westinghouse Electric Corporation. Recipient of this data has a duty to inquire of EPRI and/or Westinghouse as to the uses of the information contained herein that are permitted.

NOTICE 3: The data in this document is proprietary and confidential to Westinghouse Electric Corporation and/or its Contractors. It is forwarded to recipient under an obligation of Confidence and Trust for use only in evaluation tasks specifically authorized by the Electric Power Research Institute (EPRI). Any use, disclosure to unauthorized persons, or copying this document or parts thereof is prohibited except as agreed to in advance by EPRI and Westinghouse Electric Corporation. Recipient of this data has a duty to inquire of EPRI and/or Westinghouse as to the uses of the information contained herein that are permitted. This document and any copies or excerpts thereof that may have been generated are to be returned to Westinghouse, directly or through EPRI, when requested to do so.

NOTICE 4: The data in this document is proprietary and confidential to Westinghouse Electric Corporation and/or its Contractors. It is being revealed in confidence and trust only to Employees of EPRI and to certain contractors of EPRI for limited evaluation tasks authorized by EPRI. Any use, disclosure to unauthorized persons, or copying of this document or parts thereof is prohibited. This Document and any copies or excerpts thereof that may have been generated are to be returned to Westinghouse, directly or through EPRI, when requested to do so.

NOTICE 5: The data in this document is proprietary and confidential to Westinghouse Electric Corporation and/or its Contractors. Access to this data is given in Confidence and Trust only at Westinghouse facilities for limited evaluation tasks assigned by EPRI. Any use, disclosure to unauthorized persons, or copying of this document or parts thereof is prohibited. Neither this document nor any excerpts therefrom are to be removed from Westinghouse facilities.

EPRI CONFIDENTIALITY / OBLIGATION CATEGORIES

CATEGORY "A" — (See Delivered Data) Consists of CONTRACTOR Foreground Data that is contained in an issued reported.

CATEGORY "B" — (See Delivered Data) Consists of CONTRACTOR Foreground Data that is not contained in an issued report, except for computer programs.

CATEGORY "C" — Consists of CONTRACTOR Background Data except for computer programs.

CATEGORY "D" — Consists of computer programs developed in the course of performing the Work.

CATEGORY "E" — Consists of computer programs developed prior to the Effective Date or after the Effective Date but outside the scope of the Work.

CATEGORY "F" — Consists of administrative plans and administrative reports.

TABLE OF CONTENTS

TABLE OF CONTENTS (Continued)

LIST OF TABLES

LIST OF FIGURES

SUMMARY

This document presents the scaling analysis for the AP600 passive containment cooling system (PCS). The double-ended cold leg guillotine (DECLG) pipe break, which was identified in the SSAR[1] as the long term transient with the peak pressure, was selected for evaluation. The integrated structure for technical issue resolution (ISTIR), presented in NUREG/CR-5809,[2] was referred to and used in the preparation of this document. A first iteration scaling analysis was performed and documented previously.[3] Comments received from the NRC and ACRS review have been resolved and incorporated.

The major results and conclusions of this scaling analysis are:

- All phenomena have been identified and ranked in a phenomena identification and ranking table (PIRT).

- Control volume equations and closure relationships were developed for the significant phenomena and integrated into a scaling model that coupled the inside of containment to the external PCS.

- Comparison of the scaling model predictions to large-scale test (LST) results validated the completeness of the PIRT and the scaling model equations.

- The selected phenomenological models are dimensionless, scalable, and valid for application to both the LSTs and AP600.

- The LSTs with the steam source in the simulated steam generator compartment are representative of a DECLG; tests with the 3-in. diameter steam source do not represent the post-wetting phase of a DECLG.

- The LSTs had only two significant nonprototypical characteristics: restricted below-deck circulation into the steam generator compartment and an overcooled exterior. Both nonprototypicalities can be accommodated in the analytical scaling model.

PIRT Development

The PCS was separated into subsystems within containment and outside containment. The containment was spatially separated into a gas volume occupied by air and water vapor, liquid films and pools, and solid structures. In order to facilitate modeling and analyzing the system performance within these subsystems, phenomena were studied within discrete time intervals. Phenomena ranged from very high mass and energy releases into containment during the 30-second blowdown phase to orders-of-magnitude lower mass and energy release rates into containment during a post-blowdown phase.

A PIRT was developed, which identifies the important phenomena that must be modeled to predict the PCS performance during design basis accidents (DBAs).

Scaling Model

Control volume and constitutive relationships were developed and nondimensionalized to examine the
[
                                                                    ]^{a,c} An independent scaling model of
the PCS was developed from the [   ]^{a,c} equations, including all phenomena identified
as important in the PIRT. Results from the scaling model predict a transient pressure history nearly
identical to that of recent WGOTHIC calculations[4] and steady-state results nearly identical to
measurements from the large-scale test. Validation of the scaling model by comparison to the LST
results confirms that the PIRT is complete.

Internal Phenomena

The containment operates as a system with a nearly adiabatic exterior until 11 minutes into the
transient, consistent with the conservative assumption that the external cooling water does not exist
until 11 minutes. The exception to an adiabatic containment prior to the application of external water
is a relatively small amount of convective and radiative heat rejection from the shell. Although the
exterior is nearly adiabatic, extensive heat and mass transfer occurs between the containment
atmosphere and internal heat sinks.

The liquid film was determined to have a thermal resistance that is negligible compared to the thermal
resistance of the gas boundary layer, and the heat capacity of the thickest liquid films are negligible
compared to that of the structures they form upon. The heat and mass transfer interaction between the
IRWST surface and the containment atmosphere is insignificant. The pool of break fluid in the
bottom of the reactor cavity and steam generator compartments has such a small surface area that its
interaction with the containment atmosphere only becomes significant after approximately one hour,
when the containment temperature is dropping. After one hour, the break pool contributes slightly
more than 10 percent of the source steam.

The solid structures were determined to have a major interaction with the gas volume, acting as
significant heat sinks from the end of blowdown until well after the external cooling water starts up.
The heat sinks include steel and concrete, the steel existing in many different thicknesses (and hence,
time constants), nearly all of which have Biot numbers small enough to model as lumped masses. The
concrete has a high Biot number and requires a carefully nodalized thermal model to predict its
transient response. The steel heat sinks limit the peak pressures at the end of blowdown and up to
approximately 1500 seconds when the steel is saturated. The concrete heat sinks remain active until
much later and have a major impact on heat removal well beyond the initiation of external water.

External Phenomena

The scaling analysis shows that the PCS modeling requires three distinct external surface areas. The containment surface must distinguish between wet and dry areas because the surface temperatures and heat fluxes are different. The wet area must further be separated into subcooled liquid film and evaporating film areas. External evaporation from the shell accounts for approximately[ ]percent of the post-wetting heat removal from containment, convective heat transfer for[ ]percent, subcooled liquid for[ ]percent, and radiation for[ ]percent. The flow rate of external cooling water is the primary factor limiting external heat removal, with the air flow rate through the PCS a major factor in how much of the cooling water evaporates.

The heat transfer to the downcomer is less than 30 percent of the sensible heat transfer to the riser. The buoyancy in the downcomer accounts for less than 10 percent of the total buoyant pressure in the PCS air flow path. Because the energy input to the downcomer is small and the momentum is insignificant, modeling the downcomer in the AP600 model does not warrant more attention than the same careful application of form and friction losses and mixed convection and radiation heat transfer models as used for the remainder of the PCS model. Because the presence of the downcomer has little effect on AP600, and is easily modeled analytically, the absence of a downcomer in the LST is not significant.

LST Scaling

Application of scaling ratios to the LST and AP600 show that the LSTs provide a good simulation of the post-wetting AP600 condensation and evaporation mass transfer. [

a,c

1.0 INTRODUCTION

This report presents the scaling analysis and methodology for the AP600 passive containment cooling system (PCS). The scaling analysis was performed to identify the phenomena necessary for accurate predictions of pressure within the AP600 containment during a design basis accident (DBA) and to permit a scaled comparison of the large-scale tests to the AP600.

A first iteration on the scaling analysis was previously provided[3] to the NRC to support the preparation of the Draft Safety Evaluation Report, and comments were received and incorporated in this report. This report extends scaling [to the outside of containment]^{a,c} and scales the large-scale test (LST). This report is part of an overall schedule of meetings and reports being supplied to the NRC in support of the containment portion of AP600 design certification.

This document follows the integrated structure and technical issue resolution (ISTIR) and scaling methodology for severe accident technical issue resolution consistent with NUREG/CR-5809.[2] The subject is the AP600 PCS during a double-ended cold leg guillotine (DECLG) rupture.

2.0 SAFETY ISSUE ACCIDENT SPECIFICATION AND PHENOMENA EVALUATION

2.1 Issue and Success Criteria

Domestic U.S. nuclear reactor designs include containment to limit the release of radionuclides to the environment during a postulated breach in either the primary reactor coolant system, or the portions of the secondary cooling system inside containment. The containment is a pressure vessel designed to ASME Boiler and Pressure Vessel Code requirements for a specific design pressure. Vessel penetrations for entryways, piping, and instrumentation are sealed to limit leakage of the vessel atmosphere to the environment, even with the vessel pressure at its design limit.

A group of design basis accidents (DBAs), known as high-energy line breaks, has the potential to release significant quantities of high-temperature, high-pressure steam/water inside containment, and may increase the internal pressure to values that challenge the design pressure. Both the primary and secondary coolant systems have large values of stored energy as a consequence of the large volume, high temperature, and high pressure of their steam/water coolant and the heat capacity and high temperature of the cooling system boundaries that include the reactor vessel, steam generators, turbines, pumps, and piping.

A number of accident sequences are postulated to occur that lead to pressurization of containment. An event, such as a high-energy pipe break, will eventually lead to an increase in the containment pressure and temperature. If the break releases enough energy to containment, the containment pressure will rise and could challenge the design pressure.

The AP600 PCS has been designed to maintain containment pressure below the design pressure during a DBA without operating active containment heat removal systems and without operator action. The PCS design will be judged to be successful if, for any DBA, the PCS can:

- Maintain the peak difference between the containment pressure and the ambient pressure below 45 psig

- Reduce the pressure difference at 24 hours to less than half of the design value

2.2 Event Scenario

A DBA, such as a high-energy line break, can be postulated to occur at any time, with or without any other failures. Containments are designed with sufficient volume and strength that the initial blowdown, which releases the stored energy of the primary or secondary system, can be contained, even without significant heat rejection from the containment. Because the capacity of active or passive heat removal systems is small relative to the energy release rate during a large-break blowdown, their operation is not significant during the blowdown phase. The continued release of both core decay heat and heat from structures with long thermal time constants, such as the reactor

vessel, cause the containment pressure to continue to increase following the blowdown, although at a slower rate. In current operating plants, active systems, such as containment sprays and fan coolers, or passive systems, such as ice condensers and external containment cooling systems, are designed to reject heat at a rate sufficient to prevent the post-blowdown energy source from exceeding the vessel design pressure. This function is performed in the AP600 by the PCS.

The AP600 blowdown containment response is similar to that of existing two-loop plants. The blowdown phase of a large break lasts on the order of 30 seconds, after which the energy release rate remains below approximately 1 percent of the peak blowdown energy release rate. Following the blowdown, the containment pressure typically drops as the containment shell and other internal structures absorb some of the energy released during the blowdown. As the internal heat sinks saturate, the continued lower release rate during the post-blowdown phase may increase the containment pressure to a second peak until the source energy release rate reduces to values below the capacity of the active or passive heat removal systems. A time-pressure history[4] for AP600 is shown in Figure 2-1. For a given plant at full power, the total mass and energy released both during and subsequent to blowdown are approximately* fixed. The release rates are determined by the size of the pipe break. Generally, the larger the pipe, the more rapid the blowdown.

2.3 Nuclear Power Plant

The AP600 is the first Westinghouse design using a passive containment cooling system (PCS) to enter the licensing process. The PCS was designed to passively reject heat from containment to the ambient at a rate that will maintain the containment pressure below the design limit during the post-blowdown phase of a DBA.

The major PCS hardware includes the containment shell, the shield building, an air baffle intermediate between the shell and shield building, a 400,000 gallon water storage tank located above containment, piping from the tank to the outside center of the containment dome, and a system of weirs. The PCS system arrangement is shown in Figure 2-2.

The PCS is activated by a high containment pressure signal of 5 psi (including instrument uncertainty). The pressure signal initiates water flow from the storage tank and delivers it via piping to a bucket at the center of the dome. The bucket has weir slots that produce circumferentially uniform water application to the dome center. The water forms a thick film over the relatively flat dome with complete coverage to a radius of approximately 6 ft., where dry patches begin to appear. The water continues flowing radially outward to a radius of 22 ft. where it is collected by a weir that uniformly reapplies the water to the dome. After the weir, the film coverage is complete for some distance, then again dry streaks appear. The water continues to flow down the dome to a second weir at a radius of 50 ft. that again collects and reapplies the water uniformly around the circumference. The initially

---

* For small breaks, more energy may remain in the reactor cooling system, initiating the operation of other heat removal mechanisms, such as a steam dump to the condenser or PORV, and active reactor heat removal cooling.

complete coverage after the weir continues for some distance, then again dry streaks begin to appear. The water cools the containment by evaporation, and to a small extent by its subcooled heat capacity. The actual external film coverage is less than 100 percent, due to limits on film stability and the fact that the maximum water flow rate can be completely evaporated by approximately half the external surface area early in the transient. Evaporating 100 percent of the external film removes a fixed quantity of energy from containment regardless of the surface area. The phenomenological model for film coverage is discussed in separate documents.[5,6]

Outside air is drawn into the shield building air inlets by buoyancy and density-induced free convection. The air flows through the downcomer annulus, formed by the shield building on one side and the baffle on the other. The shield building is a 2- to 3-ft. thick concrete structure, and the baffle is formed from [   ][a,b] sheet, supported by stand-offs attached to the containment shell. At the bottom of the downcomer, the air flow turns 180 degrees and flows upward through the annular riser formed by the baffle on one side and the vessel on the other. The riser air and evaporated water vapor flow over the top of the vessel and exit through a short circular chimney.

2.4 Accident Path

With the reactor core at rated power, a high energy line is postulated to break, releasing saturated steam and water to containment. It is assumed that none of the active containment heat removal systems operate. The break is a double-ended cold leg guillotine (DECLG) rupture of the reactor cooling system piping in a steam generator compartment that vents to the containment through the top of the steam generator compartment. The 22-in. inside diameter cold leg pipe is the second largest diameter pipe in the primary system, but produces a higher second pressure peak than a hot leg (31-in. inside diameter) break. The reason is the flow resistance from the reactor to the break is less for the hot leg, so less of the reflood coolant goes through the steam generator. Consequently, the steam generator stored energy is released much more slowly over a period of many hours by convective heat transfer to the containment atmosphere. For a cold leg break, more of the steam generator stored energy is released earlier by means of blowdown and accumulator water.

The DECLG blowdown releases approximately 6,000 ft.^{3} of water to containment. Following blowdown, the accumulators force their inventory of 3,400 ft.^{3} of water through the core, followed by the core makeup tank inventory of 4,000 ft^3. The in-containment refueling water storage tank (IRWST) then provides a gravity flow of water into the core from its initial 70,850 ft.^{3} inventory. Approximately 40,000 ft.^{3} from these water sources fills the reactor cavity and lower portions of the steam generator compartments and covers the reactor to the hot and cold leg piping elevations, effectively flooding the core through the break. Continued steam generation by the reactor condenses on the externally cooled containment shell, and the condensate flows back into the IRWST. The operating deck is sloped to return all above deck condensate to the IRWST, which drains into the core.

2.5 Phenomena Identification and Ranking

The PCS can be partitioned spatially and temporally to facilitate identification of important phenomena. The PCS is partitioned into two subsystems, representing the volume within containment and the volume outside containment (the cooling air system). These two subsystems interact through the containment shell. The volume within containment can be further subdivided into as many modules as required to represent the above deck, open, dead-ended, and active (break) volumes and compartments. The air cooling subsystem comprises two modules, representing the downcomer and the riser. The modules may interact with each other and with the environment by both thermal conduction through solid boundaries and convective transport through openings. For example, the downcomer and riser are physically connected at the bottom and, in addition, interact with one-another through the baffle and with the environment through the air inlets and chimney. The compartments within containment can interact by conduction and convection and with the air cooling system by conduction.

All modules, both inside and outside containment, have common characteristics in that they encompass volumes of differing size and shape with constituents that include air, water, steel, and concrete. The steel exists as internal heat sinks and as boundary heat sinks. Internal heat sinks only interact with the air and water of a single module. Boundary heat sinks interact with the environment or with other heat sinks. The concrete is so thick that on a time scale of less than one day, any interactions through the concrete with the environment or with other modules is insignificant. Concrete can be considered as only an internal heat sink with an initial temperature. It is possible to define the "basic module" presented in Figure 2-3. Additional characteristics of the basic module are:

- The configuration of the air and water vapor are determined by the bounding solid structures and liquid interfaces

- Liquid water exists as pools and as a film on surfaces

- Steel and concrete structures are modeled as plates with one-dimensional transient heat transfer

- The fields of the gas phases are characterized by mass, energy, and momentum conservation

- The liquid film and pools are characterized by mass and energy conservation

- The solid structures are characterized by energy conservation

This phenomena identification and ranking is based on a three-module configuration, with one module encompassing the internal containment volume and the other two modules representing the downcomer and riser.

Events that occur in the containment volume are separated into two temporal phases, representing blowdown from 0 to approximately 27 seconds and post-blowdown for all subsequent time. Events that occur in the cooling air system can be separated into two temporal phases: the dry phase prior to the establishment of steady-state external cooling water flow at approximately 11 minutes and all subsequent time. It is assumed that it takes 11 minutes after the break until the external containment surface is covered by the liquid film.

The PCS makes AP600 distinctly different than conventional pressurized water reactors with steel-lined reinforced concrete containments, but the differences are not significant until the post-wetting phase. That is when the external cooling processes begin to influence the inside of containment. Consequently, the focus of this scaling analysis is on the post-wetting phenomena. The phenomena identification and ranking table (PIRT) is presented in Table 2-1 for the post-wetting phenomena. The rationale for the ranking is presented is Section 2.5.1.

2.5.1 Rationale for Phenomena Ranking

The scaling model of AP600 includes the phenomena listed as high or medium importance, with the exception of the * items in Table 2-1. A key assumption in the scaling model is that of a "well-mixed containment" that eliminates the need to include some of the phenomena effecting the module volume. Modeling details of the expected variations within containment due to jets, plumes, buoyancy, mixing, and entrainment requires a model with a level of calculational detail within the control volume (or module volume) beyond the scope of a scaling analysis. Furthermore, the expected condition in AP600 is well-mixed, due to the high entrainment rates of the buoyant plume in the break compartment. Consequently, the scaling model developed and employed for this scaling analysis does not attempt to resolve internal velocity and concentration fields. The limits of applicability of the well-mixed scaling model are discussed in Section 6.3. The scaled comparisons to the large-scale tests in Section 8.0 quantify the consequences of the well mixed assumption.

Two Component Compressible Gas

The containment atmosphere is steam and air and is compressible throughout the transient. The steam and air fractions are very important to the mass transfer relationships and must be known at the wet surface and in the bulk fluid to predict mass transfer rates. Outside containment post-wetting, compressibility is not important, but evaporation into the riser makes the steam and air fractions important at the wet surface and in the bulk fluid. The downcomer is only exposed to ambient air with convective heat transfer and can be considered as a single-species gas.

Jets

Forced jets vigorously mix and entrain the AP600 containment atmosphere during blowdown. By entraining large volumes of air from the break room, forced jets induce a large volumetric air flow

through all the interconnected rooms, thereby including the below deck regions in the well-mixed containment. Post-blowdown jets are buoyant, rather than forced.

Buoyant Plumes

Buoyant plumes mix and entrain the AP600 containment atmosphere after blowdown. The plume source in the steam generator compartment entrains below deck atmosphere, which induces flow through the interconnected compartments, promoting overall containment circulation and maintaining the well-mixed containment. Post-blowdown is the primary phenomena responsible for the well-mixed containment assumed in the scaling model. Buoyant plumes do not occur outside containment.

Buoyancy

Buoyancy due to temperature and molecular weight differences is responsible for the post-blowdown free convective air flow rate in the downcomer and riser, and induces riser air velocities high enough for forced convection heat and mass transfer. Temperature- and molecular-weight-induced buoyant phenomena also induce the negatively buoyant boundary layers that give rise to free convection on the inside of containment.

Jet-Plume Mixing/Entrainment

The effect of jet- and plume-induced mixing and entrainment is to produce a well-mixed containment throughout the transient. No other effects have been included in the scaling model.

Steam Source Superheating

Superheating is not important because the energy transfer models separately consider convective heat transfer (based on temperature difference) and mass transfer (based on steam partial pressure difference). The moderately greater source temperature in the tests (up to 330°F) compared to the AP600 source at saturation temperature produces only a few percent increase in the source energy.

Flow Field Stability

There are no indications of either internal or external flow field instabilities that could effect containment temperature or pressure. The scaling analysis in Section 7.0 shows that heat transfer and momentum in the downcomer, relative to the riser, is so small that the possibility of downcomer instabilities is insignificant.

Liquid Film Heat Transfer

An important aspect of heat transfer to the liquid film is the liquid enthalpy that is carried away by the liquid films on both the inside and outside of containment as they drain off. This is not the same as

heat transfer to the subcooled film, discussed under "Liquid Film Stability." The maximum internal and external film thicknesses are approximately [   ] with corresponding heat transfer coefficients of approximately [   ] BTU/hr-ft.^{2}-°F. Although considered of low importance, this heat transfer coefficient was included as a constant in the scaling model. Liquid thickness and heat transfer in AP600 and the large-scale test (LST) were compared and are documented separately.[7]

Liquid Film Stability

Liquid film stability is an important consideration that has been extensively analyzed and documented[5,6]. References 5 and 6 document the expectation that all of the supplied external water is evaporated for the period of time covered by this scaling analysis, which greatly simplifies the scaling analysis.

Liquid Film Subcooling

The externally supplied liquid film has heat capacity by virtue of being supplied at a temperature lower than the temperature at which the film evaporates. This subcooled liquid heat capacity is shown in Section 7.0 to account for approximately [   ] percent of the post-wetting heat removal from AP600 and thus, is [   ] The higher scaled external flow rates in the LST make this somewhat more of a concern for the test and an aspect of the test that must be carefully examined. Thus, the phenomena cannot be neglected and is elevated to moderately important.

Free-Convection Heat Transfer

Velocity fields inside containment are forced-convection dominated during the early portion of blowdown, and free-convection dominated thereafter. Although free-convection heat transfer is not significant in comparison to mass transfer, the free-convection mass transfer coefficient is calculated from the heat transfer coefficient, so free-convection heat transfer is modeled. During blowdown, the free-convection heat transfer correlation gives a conservatively low estimate of total heat transfer. Outside containment post-blowdown, convective heat transfer to the riser and downcomer air is the dominant source of sensible heating to drive the buoyant air flow. Although the air flow is natural convection, the resulting downcomer and riser air flows are channel flows with both free- and forced-convection characteristics. In the riser, forced-convection heat transfer always dominates, so free convection is not important. In the downcomer, heat transfer is mixed free and forced convection, so free-convection heat transfer is important there.

Forced-Convection Heat Transfer

Velocity fields inside containment are forced-convection dominated during the early portion of blowdown, and free-convection dominated thereafter. Furthermore, with mass transfer present during blowdown, convective heat transfer is negligible. Consequently, inside containment forced-convection heat transfer can be considered unimportant. Forced-convection heat transfer is always important in

the riser and downcomer as the major source of sensible heat transfer and thus, is the major inducer of the buoyant air flow.

Radiation Heat Transfer

Temperature differences within containment are small enough that radiation heat transfer rates are low. In comparison to the condensation mass transfer that is always present within containment, radiation is negligible. Outside containment radiation is a major source of energy transfer to the baffle and shield and, therefore, is important in the riser and downcomer[7] for both wet and dry surfaces during post-blowdown.

Free-Convection Mass Transfer

Inside containment, mass transfer is the only important mechanism for energy transport from the containment atmosphere to the internal heat sinks and containment surface. Except for blowdown, internal velocities are low enough that free convection dominates forced convection. During blowdown, free convection mass transfer provides a conservatively low estimate of the mass transfer rate. Outside containment, mass transfer occurs between the wetted shell and the riser air flow. At the times of interest to external heat transfer, the air velocities in the riser are always high enough to produce forced convection heat transfer, so by analogy, free-convection mass transfer does not exist outside containment.

Forced-Convection Mass Transfer

Forced-convection mass transfer is important internally during blowdown, but is replaced by free convection thereafter. Outside containment, forced-convection mass transfer is important in the riser post-wetting due to the forced-convection dominated air flow.

One-Dimensional Transient Conduction Heat Transfer

The majority of heat sinks and the containment shell are large, flat-surfaced solids that may be modeled with one-dimensional heat transfer. Because the heat sinks and shell heat flux are so important, one-dimensional transient conduction heat transfer is important. One-dimensional conduction to the sinks and through the shell is important from blowdown to the end of the transient.

Two- or Three-Dimensional Conduction

Calculations have shown that circumferential conduction in the shell at the edge of the wet/dry regions causes a small local increase in the heat transfer through the shell relative to one-dimensional conduction. This effect was neglected as an acceptably small underprediction of heat transfer.

Inter-Module Convection

As the containment shell and baffle heat up after blowdown, significant convective air flows develop between the riser and downcomer, making this effect important.

Inter-Module Conduction

Inter-module conduction is important after wetting between the containment shell and riser and between the riser and baffle. Prior to wetting, it is moderately important through the shell to supply the radiant and convective heat loss from the shell, and through the baffle to supply the radiation to the shield and convection to the downcomer. Inter-module conduction is not important during blowdown.

Form and Friction Losses

The form and friction losses are the major flow resistances in the riser and downcomer air flow path and are important for air flow rate predictions. Form and friction losses are not required in the single volume containment portion of the scaling model.

a,c

Component	Phenomena	Ranking		
Module Volume	Two component compressible gas Jets Buoyant plumes Buoyancy Jet-plume mixing/entrainment Steam source superheating Flow field stability			
Module Surface	Liquid film heat transfer Liquid film stability Liquid film subcooling Free convection heat transfer Forced convection heat transfer Radiation heat transfer Free convection mass transfer Forced convection mass transfer			
Module Solids	One-dimensional transient conduction heat transfer Two or Three-dimensional conduction			
Inter-Module	Convection Conduction Form and friction losses			

TABLE 2-1
PCS POST-WETTING PHENOMENA IDENTIFICATION
AND RANKING TABLE
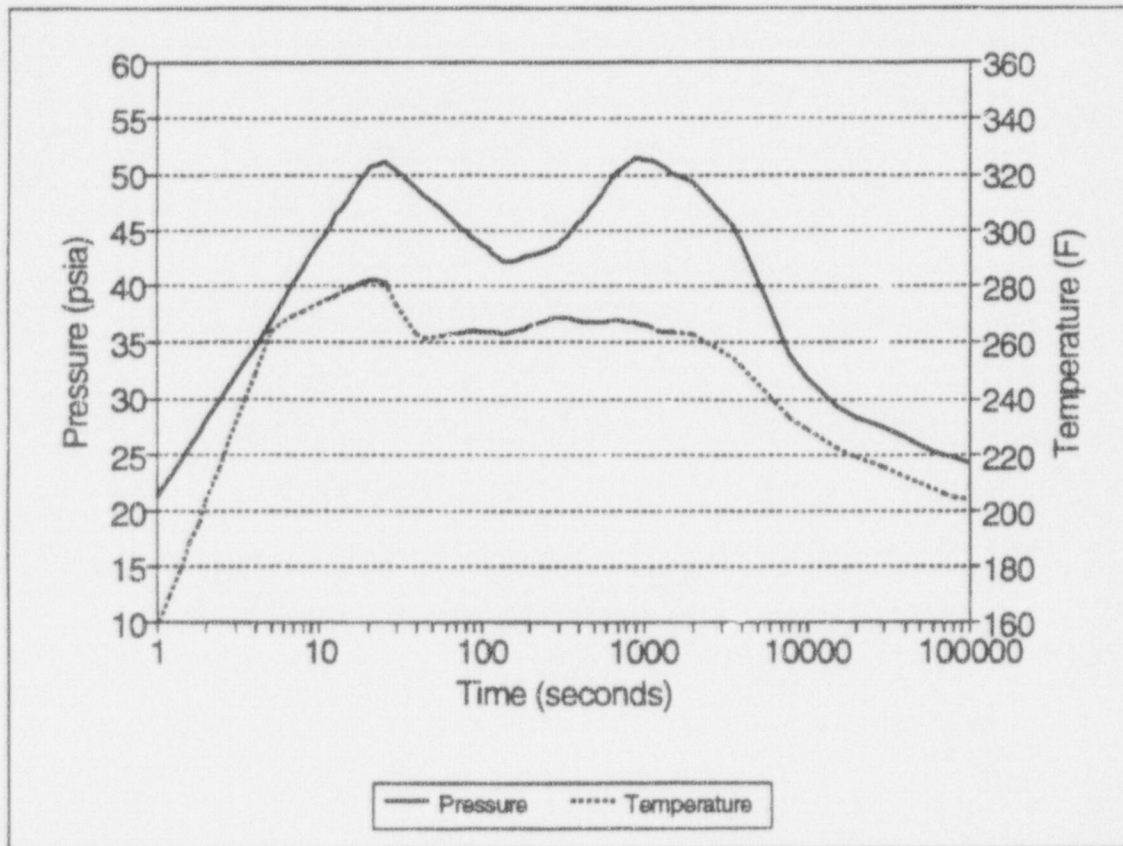
Figure 2-1 Pressure and Temperature Histories during a DECLG

PCS Water
Storage Tank

Air
Inlet

Air
Inlet

Steel
Containment
Vessel

Concrete
Shield
Building

Air Flow
Baffle

AP600 Ultimate
Heat Sink

AP600C10.eps
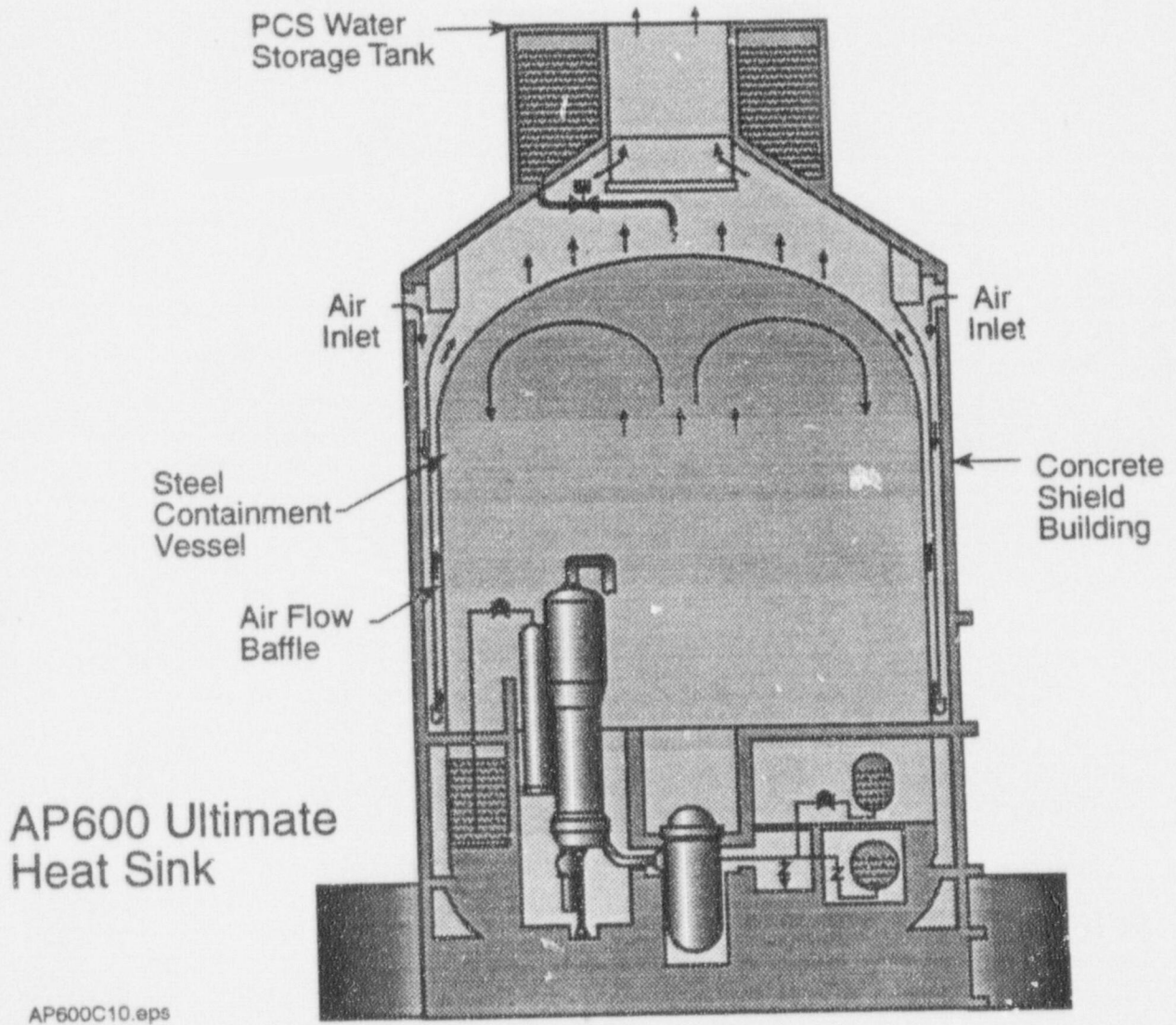
Figure 2-2 PCS System Arrangement

Figure 2-3 Module Decomposition and Architecture

Module

Constituent   Air/Vapor   Water   Solids

Phase   Boundary Layers   Liquid   Steel   Concrete

Geometry   Pools   Films   Plate   Plate

Field

M   E   E   E

M   E   MM   M   E

M = mass
E = energy
MM = momentum
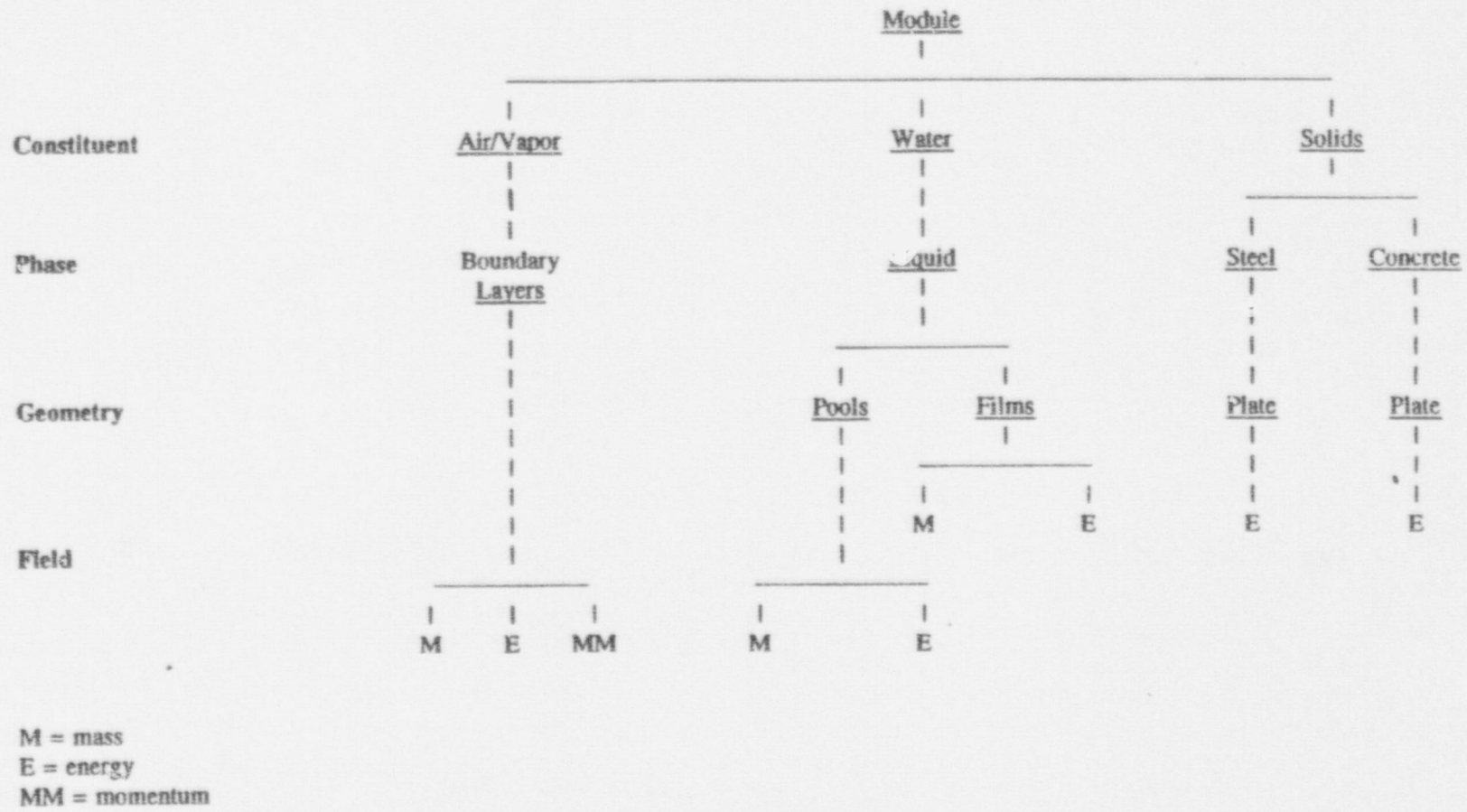
3.0 SCALING METHODOLOGY

The scaling methodology described in NUREG/CR-5809 was followed for scaling AP600. The principle steps were:

- Develop control volume, interface and closure equations based on the phenomena identified in the PIRT to model the AP600 containment and PCS

- Apply the scaling model to AP600 to determine the important phenomena

- Validate the scaling model by comparison to test results and computer models, and iterate with the PIRT and the scaling model development to obtain closure

- Scale the large-scale tests to AP600

- Identify limits to the validity of the scaling model

3.1 General Characteristics

A schematic of the inside of containment is shown in Figure 3-1, and the outside of containment is shown in Figure 3-2. Prior to developing the control volume equations necessary to characterize the PCS, some important characteristics are noted to better understand the modeling approach.

Break Mass and Energy Source

There is a single mass and energy source (the break) and no mass transfer out of containment. All the energy added to containment from the break will be stored in internal heat sinks and/or transferred by conduction through the containment shell and rejected to the atmosphere.

The volumetric, mass, and energy flow rates of steam and water are shown respectively in Figures 3-3, 3-4, and 3-5. The total mass and energy release rates are those presented in the SSAR for the DECLG. The containment pressure calculated by $\underline{W}$GOTHIC[4] for the DECLG was used to determine the fraction of break flow that was released as saturated steam and saturated water. The figures each show the blowdown that is terminated at 27 seconds, followed by approximately 3 seconds with no break flow while the accumulators refill the reactor. Following refill, the high accumulator injection flow rate quickly produces a significant primary system overcooling by saturated liquid. This saturated liquid (with little vapor) displaces very little volume and thus, effectively cools the reactor without pressurization of containment.

Following the emptying of the pressurized accumulators at 150 seconds, the core makeup tank flow begins, initially exiting the break with very high steam quality, resulting in an increase in containment pressure. The core makeup tank flow is followed at 1,404 seconds by the IRWST flow, which

continues indefinitely due to condensate drainage back to the IRWST and the break pool level, which by approximately 80,000 seconds covers the break.

External Surface

The external containment surface is assumed to be dry until 11 minutes into the transient, although external water flow is initiated within a few seconds of the event. Prior to 11 minutes, heat rejection from the exterior of containment is conservatively assumed to be only by convection to the buoyant air in the riser and radiation to the baffle. The peak containment exterior surface temperature occurs just prior to the initiation of external cooling water. The application of external cooling water cools the containment outer surface by its subcooled heat capacity and by evaporation. At the initial maximum water flow rate, the water film completely covers the dome at the weirs, but as discussed in the wetting stability report,[5,6] the film may separate into alternate wet regions with narrow dry stripes between. The dry regions do not widen significantly until 18,000 seconds into the transient when the external water supply rate is reduced. Both wet and dry surface regions coexist for the duration of the transient.

The model of the containment surface must distinguish between wet and dry areas because the surface temperatures and heat fluxes are different. The wet area must further be separated into subcooled and evaporating areas because the heat flux from the inside of containment to the subcooled and evaporating areas are quite different in magnitude. An example will help illustrate the magnitude.

The heat sink for heat transferred from inside containment can be either the subcooled liquid on the outside, or evaporation to the riser air. Typical heat transfer coefficients between the inside and outside of containment are 100, 1000, 200, 1000, and 50 BTU/hr-ft.^{2}-°F, respectively, for the condensation, internal liquid film, shell, external film, and evaporation. Given these values, the equivalent heat transfer coefficient is [ ]^{a,c} for heat transfer to the external film and [ ]^{a,c} for evaporation to the riser air. For the same temperature difference, the subcooled heat flux will be approximately twice the evaporating heat flux, so it is appropriate to model subcooled and evaporating regions of containment separately.

The subcooled model employed in this scaling analysis assumed that the subcooled film is heated from its source temperature to the temperature of the evaporating film. The subcooled area is the quantity of surface required to heat the cooling water to the temperature of the evaporating film without evaporation, convection, or surface radiation. The subcooled film is assumed to be at the average of its source and evaporating temperatures for calculating the conduction heat transfer from the shell. Once raised to its evaporating temperature the water no longer has subcooled heat capacity and all heat is released from the film at its surface temperature by evaporation, convection, and radiation. A more detailed description of the equations is presented in Section 4.0, and examples are presented in Appendix C.

Scaling of External Phenomena

The time of interest for the external scaling analysis is beyond 2,000 seconds. By this time, the cooling air system has gone through its initial heatup and, because of the low heat capacity of the riser, baffle, and downcomer, these external components can be modeled as quasi-steady. Assumptions discussed in Section 4.3.3 allow the shield building to also be modeled with simplified steady-state equations, even with its large heat capacity. Thus, although the conservation equations are derived for transient conditions, the steady-state form of the equations may be used for external scaling, allowing a simplified form of the control volume equations to be used. The control volume equation development and steady-state equations are presented in Appendix A.
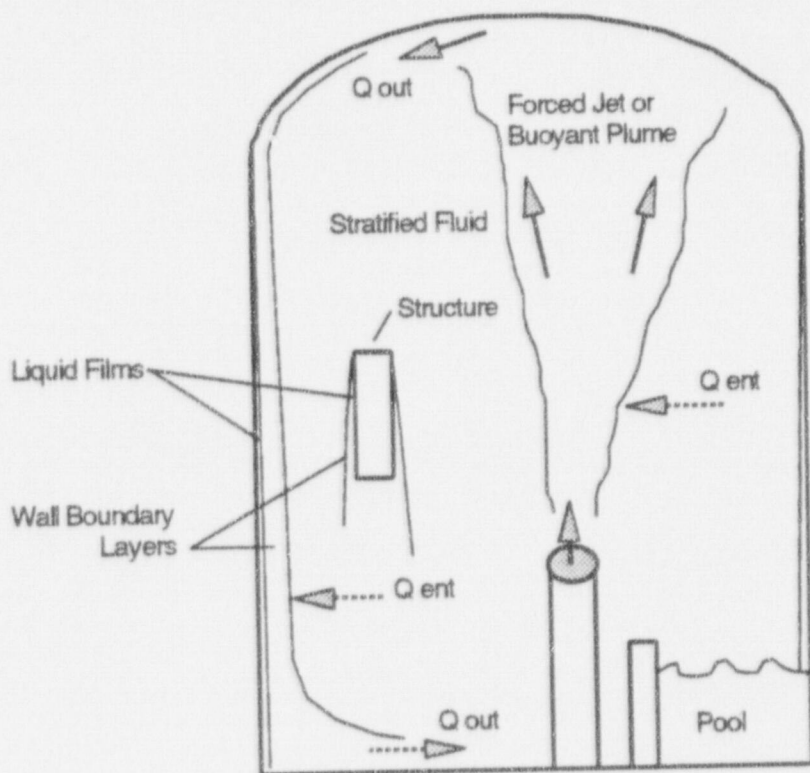
Figure 3-1 Schematic Model of AP600 Inside Containment

Chimney Height 51 ft.

Riser Height 121 ft.

Downcomer Height 107 ft.

Shell

Baffle

Shield
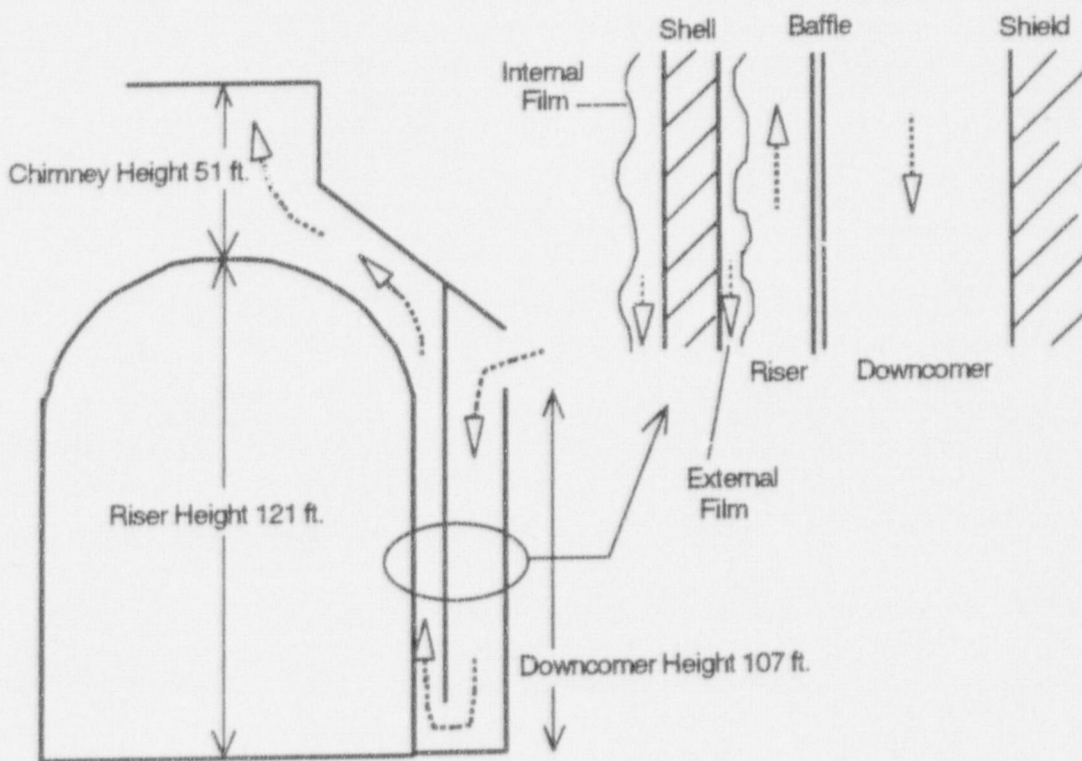
Internal Film

Riser

Downcomer

External Film

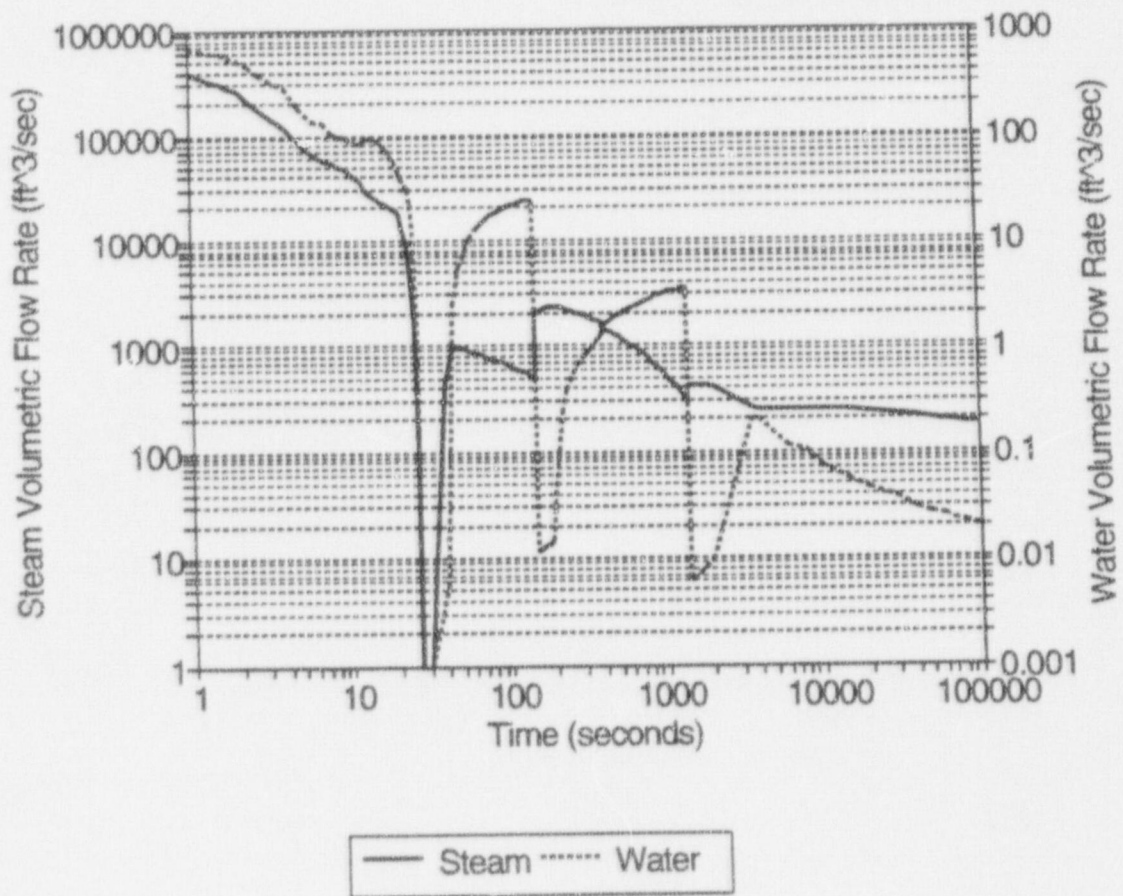Figure 3-2 Schematic of AP600 Showing Outside of PCS

Figure 3-3 Steam and Water Break Volumetric Flow Rates during a DECLG
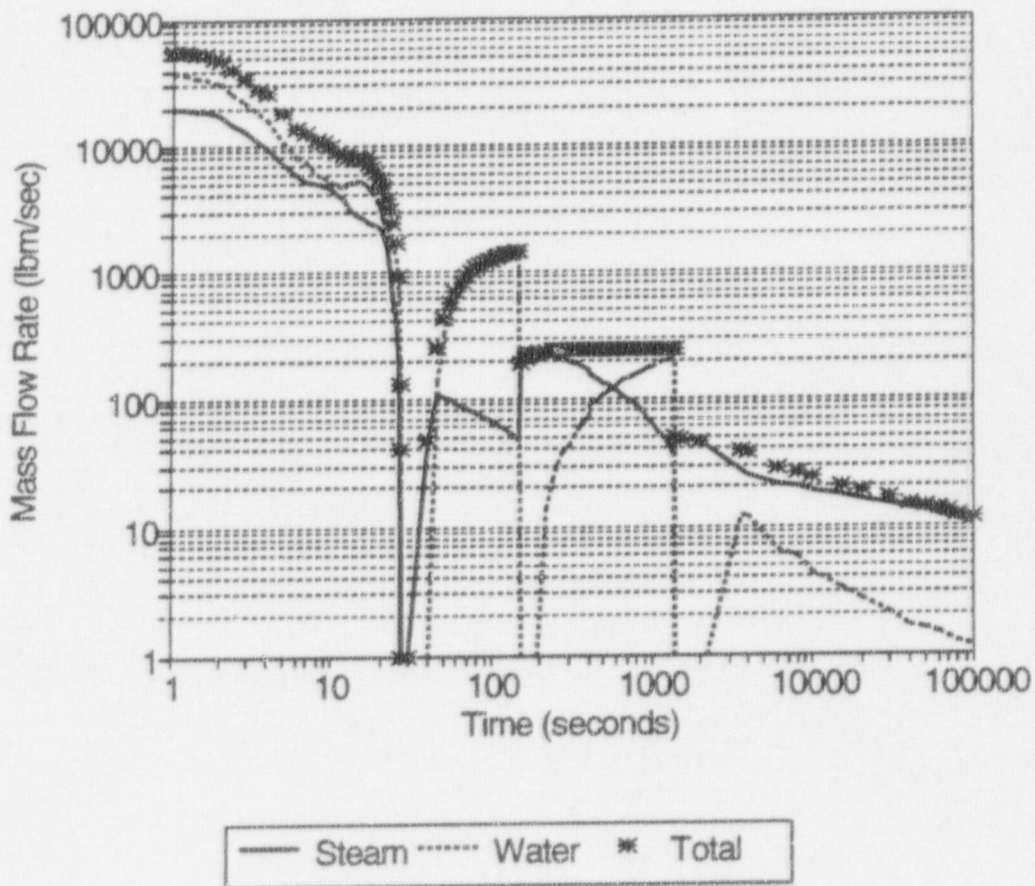
Figure 3-4 Steam and Water Break Mass Flow Rates during a DECLG
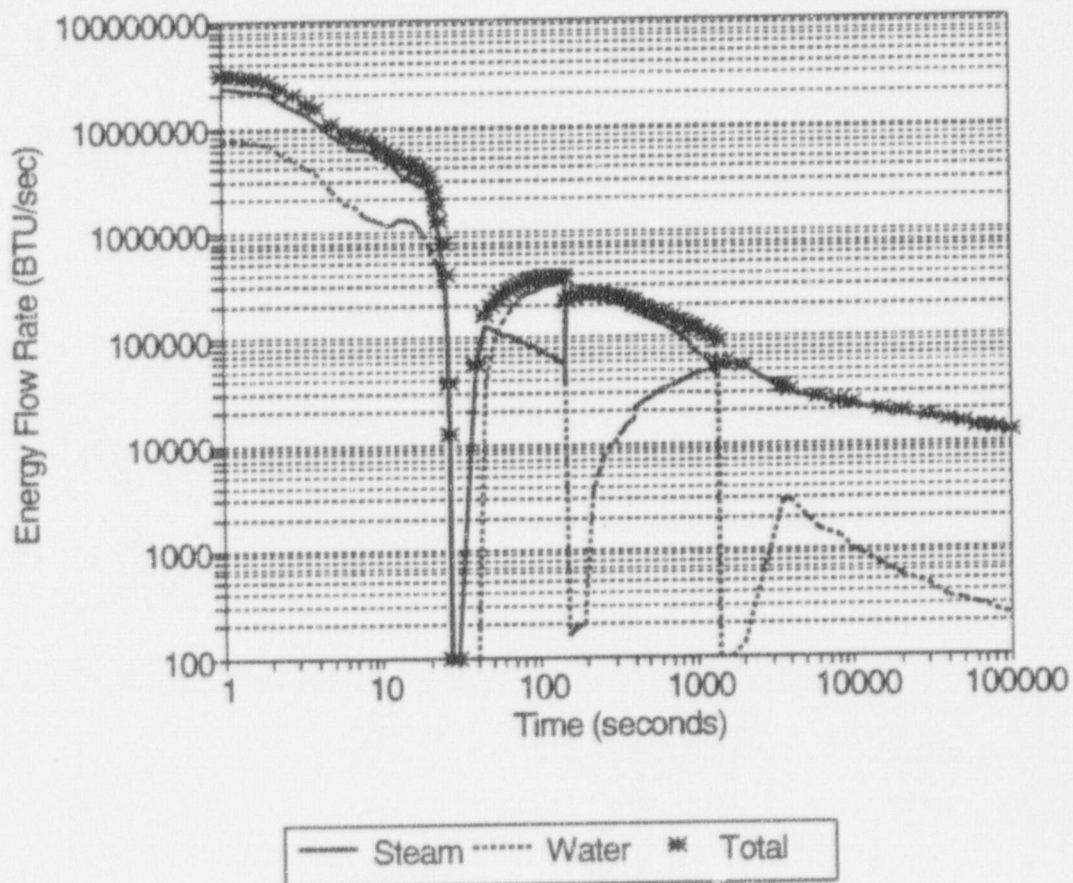
Figure 3-5 Steam and Water Break Energy Flow Rate during a DECLG

4.0 PCS CONTROL VOLUME EQUATIONS

The control volume equations for the inside of containment and the equations that couple the inside of containment with the riser, baffle, downcomer, and shield are presented in this section, along with the resulting nondimensional ratios. Additional information on the development of the control volume equations and the derivation of the pi groups by nondimensionalizing the control volume equations is presented in Appendix A. Interface equations that are required to couple the control volume equations are also presented.

4.1 Containment Gas Control Volume

The time constant for containment atmosphere (volume/volumetric flow rate) during blowdown is a few seconds. This high flow rate and high velocity jet have the effect of thoroughly mixing the entire above-deck atmosphere. The hydraulic network model (from WGOTHIC) predicts that during blowdown the break compartment pressurizes and forces very high flow rates through all of the interconnected compartments leading to the main steam volume above deck. The air/vapor volume and volume fractions of the containment compartments are presented in Table 4-1. This forced steam flow produces a steam-rich atmosphere throughout the below-deck compartments during blowdown. Following blowdown, the low-density steam source rises from the steam generator compartment as a buoyant plume, creating a low-static pressure in the break compartment that entrains the atmosphere from surrounding compartments and continues to induce significant convection through all of the interconnected compartments. The result is that most of the lower compartments do not develop the low-steam/high-air concentrations that would develop from stratification, due to the continual circulation of the above-deck atmosphere through the lower compartments to the low-pressure entraining flow in the break compartment. Consequently, the entire containment, including lower compartments, is well mixed both during blowdown and over the long term when the PCS is operating.

The containment atmosphere interacts with liquid films and pools, and is driven by a single steam source. Although boundary layers exist on each structural component, large and small, the structures were grouped into six categories, as explained in Section 4.3.1 of this report, to reduce the large number of structures to a manageable number. The water source is input to the pool.

The containment steam and air mass conservation equations can be written:

$$\frac{dm_{ct,stm}}{dt} = \dot{m}_{stm,in} - \sum_{i=1}^{6} \dot{m}_{ct-lf,i} + \dot{m}_{ct-pl} - \dot{m}_{ct-rw}$$

$$\text{and} \quad \frac{dm_{ct,air}}{dt} = 0$$

(1)

TABLE 4-1
PCS CONTAINMENT AIR/VAPOR VOLUMES AND VOLUME FRACTIONS

Region	Volume (ft³)	Vol Frac
		a,c
Above Deck		
Reactor Cavity		
Accumulator		
Accumulator		
Steam Generator		
Steam Generator		
CMT and CVCS		
Refueling Cavity		
IRWST		
Total		

and the energy equation:

$$\frac{d}{dt}(mug)_{ct} = (\dot{m}hg)_{stm,in} - hg_{ct,stm}\sum_{i=1}^{6}\dot{m}_{ct-lf,i} + hg_{pl,stm}\dot{m}_{pl-ct} - hg_{ct,stm}\dot{m}_{ct-rw}$$
$$- \sum_{i=1}^{6}h_{lf,i}A_{ct-lf,i}(T_{ct}-T_{lf,surf,i}) + h_{pl}A_{ct-pl}(T_{pl,surf}-T_{ct}) - h_{rw}A_{ct-rw}(T_{ct}-T_{rw,surf}) \tag{2}$$

Appendix B presents a process by which Equations (1) and (2) can be put in the following form with the time rate of change of pressure as the dependent variable:

a,c

$$\tag{3}$$

An equation of state for the gas is also required, in addition to Equations (1) and (3), to solve for pressure. The gas volume, V_{ct}, is not a constant; it reduces due to displacement by the addition of liquid water from the break and leads to pressurization of containment according to Equation (3). However, the total water added to the control volume (not just moved around within the control volume) is only 13,400 ft^3 out of 1,786,300 ft^3 (0.7 percent) and is neglected in the scaling model.

Equation (3) was made dimensionless by dividing by reference values of flow rate, density, volume, area, pressure, temperature, heat transfer coefficient, and mass transfer coefficient (see Appendix A for examples). Each term of each equation was then divided by the steam source term, $\dot{m}c_pT$, to produce the normalized equations that define the time constants and pi groups. The resulting time constants and pi groups are defined in Table 4-2.

4.2 Liquid Control Volumes

The water sources inside containment consist of the primary system, the IRWST, the two core makeup tanks, and the two accumulators. The primary system water (6,000 ft.^{3}) is lost during blowdown at 27 seconds, followed by the accumulator water (3,400 ft.^{3}) from 27 to 150 seconds, the core makeup tank water (4,000 ft.^{3}) from 150 to 1,404 seconds, and the IRWST (70,800 ft.^{3}) after 1,404 seconds. At 100,000 seconds the total flow from the break is approximately 40,000 ft.^{3} of total water with 1,700 ft.^{3} as vapor. As the transient progresses, the blowdown water fills the reactor cavity, flooding the bottom of the steam generator compartments at approximately 100 seconds. The water level in the reactor cavity and steam generator compartments continues to rise without flooding other areas until after 100,000 seconds (28 hours). The surface area of the pool is shown in Figure 4-1, assuming that from the total break flow, 100,000 lbm of steam pressurizes containment and the remainder floods the reactor cavity. For comparison, the surface area of the IRWST is 2,760 ft.^{2}, and the containment shell above deck is 54,116 ft.^{2} All three liquid surfaces interact with the containment gas.

Water also exists as a thin liquid film that develops on the surface of any structure that is cooler than the saturation temperature of the local atmosphere. The liquid films develop to a maximum thickness of approximately 0.005 in. at the condensing heat fluxes expected, with shorter length structures having thinner layers. With a total surface area inside containment (including the shell) of approximately 260,000 ft.^{2} the total liquid film volume can be estimated to be 108 ft.^{3} of water distributed throughout containment. The presence of the liquid film primarily represents an additional thermal resistance to heat transfer throughout the transient. The characteristics of liquid films in AP600 and in the LST have been documented[4] and the heat transfer coefficient of the film was determined to be approximately 1000 B/hr-ft.^{2}-°F.

The water source outside containment is the external cooling tank. The tank has a capacity of 400,000 gallons and has internal drain pipes of different sizes and heights to control the flow rate to approximate the external cooling requirements. The flow rate of the tank drainage is presented in Figure 4-2.

| TABLE 4-2 |
| TIME CONSTANTS AND TRANSPORT RATIOS FOR INSIDE CONTAINMENT |

a,c

The IRWST is relatively isolated from convective gas flow because it has small openings located at the same elevation. The IRWST, with its initial 4,000,000 lbm of water, will heat up slowly and is expected to stratify at the surface as the hotter condensate from the wall drains in. The IRWST, shell, and internal heat sinks will initially be at a lower temperature than the transient gas temperature due to their low initial temperatures. However, due to its small surface area, high thermal stratification, and lack of convective interaction with the containment atmosphere, it is expected to have negligible thermal and mass transfer interaction with the containment atmosphere.

The pool of break water is exposed to a relatively high forced convective flow due to its proximity to the break. The pool is supplied by break liquid at the saturation temperature at the total pressure of the containment, which is generally hotter than the ambient temperature, so the pool will evaporate to the containment atmosphere throughout the transient. (There are two brief periods when the containment atmosphere is heating rapidly and the pool is a heat sink rather than a heat source.

The liquid is separated into internal surface films, external surface films, pools, and the IRWST. The mass and energy control volume equations for each liquid type are presented in Table 4-3. An internal liquid film equation can be written for each of the six structures and, on the shell, can be further broken down into three distinct equations corresponding to the dry external region, the subcooled

external region, and the wet external region. The external liquid film covers the subcooled region and the wet region. The temperature of the subcooled region is low enough that radiation, convective heat transfer, and convective mass transfer are neglected. The area of the subcooled film is the area required to heat the subcooled film from its inlet temperature to the temperature of the evaporating film. The subcooled region film outflow is the inflow to the evaporating region. Other characteristics of the external film were discussed in Section 3.1. The pi groups for the internal liquid are included among those for the containment gas (Table 4-2). The pi groups of interest for the external film include radiation to the baffle, evaporation mass transfer, convective heat transfer, and subcooled heat:

Radiation from liquid film to baffle

$$\left[\quad \right]^{a,c} \quad (12)$$

Evaporation from external film

$$\left[\quad \right]^{a,c} \quad (13)$$

Convection from liquid film to riser

$$\left[\quad \right]^{a,c} \quad (14)$$
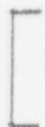
Heat transfer to subcooled external film

$$\left[\quad \right]^{a,c} \quad (15)$$

4.3 Structure Control Volumes

4.3.1 Internal Structures and Containment Shell

The structural materials consist of steel and concrete. The steel thickness ranges from 0.007 to 1.25 ft., so the structure time constants vary from approximately 10 to 5,000 seconds. The steel was separated into five groups based upon thickness: 0 to 0.0155 ft., 0.0156 to 0.051 ft., 0.052 to 0.255 ft., the shell at 0.1345 ft., and over 0.255 ft. The steel with thicknesses less than 0.255 ft. has Biot numbers less than 1, so it may be accurately modeled as lumped masses. Although the steel with thicknesses greater than 0.255 ft. is not accurately modeled as a lumped mass, the total volume of such steel is small, so the error induced by this approximation will have minor consequences. The distribution of the steel is presented in Table 4-4. The shell steel was treated as distinct because it has a cooling water source on the outside after 11 minutes.

TABLE 4-3
LIQUID CONSERVATION EQUATIONS

Mass Conservation Equations

Pool (pl)

$$\frac{dm_{pl}}{dt} = \dot{m}_{wat,in} - (\dot{m}hg)_{pl-sf} \tag{16}$$

Liquid film (lf) for each structure, i

$$\frac{dm_{lf,i}}{dt} = \dot{m}_{lf,i,in} + \dot{m}_{cond,i} - \dot{m}_{lf,i,out} \tag{17}$$

External film (xf) for subcooled and wet exterior

$$\frac{dm_{sc}}{dt} = \dot{m}_{sc,in} - \dot{m}_{sc,out} \qquad \frac{dm_{xf}}{dt} = \dot{m}_{xf,in} - \dot{m}_{evap} - \dot{m}_{xf,out} \tag{18}$$

IRWST water (rw)

$$\frac{dm_{rw}}{dt} = (\dot{m}hg)_{ct-rw} + \sum_{i=1}^{n} \dot{m}_{lf,i} - \dot{m}_{rw,drain} \tag{19}$$

Energy Conservation Equations

Pool (pl)

$$\frac{d(muf)_{pl}}{dt} = (\dot{m}hf)_{wat,in} - (\dot{m}hg)_{pl-ct} - h_{pl-ct}A_{pl-ct}(T_{pl}-T_{ct}) \tag{20}$$

Liquid film (lf) for each structure, i

$$\frac{d(muf)_{lf,i}}{dt} = (\dot{m}_{cond}hg)_{lf-ct,i} - (\dot{m}hf)_{lf,i,out} + h_{ct-lf,i}A_{ct-lf,i}(T_{ct}-T_{lf,i,surf}) - k_{lf}A_{ct-lf,i}\frac{dT_{lf,i}}{dx}\bigg|_{surf} \tag{21}$$

Subcooled external film (sc)

$$\frac{d(muf)_{sc}}{dt} = \dot{m}_{sc,in}hf_{sc,in} - \dot{m}_{sc,out}hf_{sc,out} + k_{sc}A_{sh-sc}\frac{dT_{sc}}{dx}\bigg|_{surf} \tag{22}$$

Evaporating external film (xf)

$$\frac{d(muf)_{xf}}{dt} = \dot{m}_{xf,in}hf_{xf,in} - \dot{m}_{evap}hg_{xf,surf} - \dot{m}_{xf,out}hf_{xf,out}$$
$$- h_{xf-n}A_{xf-n}(T_{xf,surf}-T_n) - \sigma\varepsilon A_{xf-n}(T_{xf,surf}^4-T_{bl}) + k_{xf}A_{sh-xf}\frac{dT_{xf}}{dx}\bigg|_{surf} \tag{23}$$

IRWST water (rw)

$$\frac{d(muf)_{rw}}{dt} = \dot{m}_{ct-rw}hg_{ct} + h_{ct-rw}A_{ct-rw}(T_{ct}-T_{rw,surf}) - \dot{m}_{drain}hf_{rw} + \sum_{i=1}^{6} \dot{m}_{lf,i}hf_{lf,i} \tag{24}$$

An energy conservation equation can be written for each of the five steel structures:

$$\frac{d}{dt}(V\rho c_v T)_{st,i} = \dot{q}_{st-lf,i} \quad \text{where} \quad \dot{q}_{st-lf,i} = -k_{st,i} A_{st-lf,i} \frac{dT_{st,i}}{dx}\bigg|_{surf} \tag{25}$$

The time constant is given by:

$$\tau_{st,i} = \frac{(V\rho c_v)_{st,i,0}(T_g - T_{st,i,0})}{\dot{q}_{st,i,0}} \tag{26}$$

Dividing the heat flow rate into the structure by the steam source energy rate produces a pi group for each structure.

$$\left[\right]^{a,c} \tag{27}$$

The concrete is much thicker, with lower thermal conductivity, so it cannot be modeled by a simple lumped parameter model. All concrete is 2 ft. or thicker; 2-ft.-thick concrete has a time constant of approximately 124 hours, so on a time scale of 1 day, the concrete temperature at a depth greater than 1 ft. remains at its initial temperature. In addition, all but a negligible fraction of the concrete is lined with 1/2-in. thick carbon steel plate. It is notable that there is relatively little concrete above deck; 94 percent of the concrete surface is below deck. The distribution of the concrete is also presented in Table 4-4.

The steel-lined concrete was modeled with a finite element model in which the element thicknesses increased from very thin at the surface to much thicker several inches in the structure. The energy conservation equation was written for each element j:

$$\frac{d}{dt}(V\rho c_v T)_j = \dot{q}_{in,j} - \dot{q}_{out,j} \tag{28}$$

The surface heat flux into the structure was coupled to the liquid film by the equation:

$$k_{lf} \frac{dT_{lf}}{dt}\bigg|_{surf} = k_{cc} \frac{dT_{cc}}{dt}\bigg|_{surf} \tag{29}$$

and the volume-to-volume connections defined by:

$$k_{cc,j} \frac{dT_{cc,j}}{dt}\bigg|_{surf} = k_{cc,j+1} \frac{dT_{cc,j+1}}{dt}\bigg|_{surf} \tag{30}$$

The pi group for concrete is defined by Equation (27) with the surface heat flux defined by Equation (29)

TABLE 4-4
DISTRIBUTION OF STEEL AND CONCRETE INSIDE CONTAINMENT

Concrete/Liner	Steel	Steel	Steel	Shell	Steel
					a,c

4.3.2 Baffle Control Volume

The baffle is made of [ ]^{a,c} thick carbon steel plate and has a time constant on the order of a few seconds. The baffle heat fluxes are low and the maximum temperature drop across the baffle is less than 0.10°F. Thus, the baffle can be approximated as an isothermal structure with no resistance to heat flow. The baffle does not have liquid films. The baffle receives radiation from the dry portions of the containment shell and from the external film. The baffle radiates to the shield building and interacts through convective heat transfer with the downcomer and riser. The steady-state energy equation for the baffle can be written:

$$\left[\right]^{a,c} \quad \text{Baffle} \tag{31}$$

Dividing each term by the steam source energy produces five pi groups, one of which was presented for the external liquid film. The four new pi groups are:

Radiation heat transfer from dry shell to baffle   Radiation from baffle to shield

$$\left[\right]^{a,c}$$

4.3.3 Shield Building Control Volume

The time constant of the 3-ft. thick shield is over two hundred hours, so on the time scale of interest, up to 24 hours, events inside and outside the shield building cannot influence each other through the shield thickness. The temperature of the shield is difficult to approximate with less than a detailed transient model of conduction from the surface to the interior. However, the solution can be simplified if it is assumed $\left[\right.$

$\left. \right]^{a,c}$ This

assumption keeps the shield temperature $\left[\right.$

$\left. \right]^{a,c}$ With that assumption, the energy

equation for the shield can be written:

$$\left[\right]^{a,c}$$

The shield energy equation gives two pi groups, one of which was previously developed from the baffle equation. The unique shield pi group represents convective heat transfer from the shield to the downcomer:

$$\left[\right]^{a,c}$$

4.4 Air Flow Path Control Volumes

The riser and downcomer make up the PCS air flow path. Ambient air is drawn into the downcomer at the air inlets, flows approximately 107 ft. to the bottom of the downcomer, turns 180 degrees and flows up the riser due to buoyancy induced by heating and evaporation within the riser. The top of containment is 121 ft. above the bottom of the downcomer and the chimney extends upward an additional 51 ft. A schematic is shown in Figure 3-2.

The riser and downcomer have similar mass, energy and momentum equations, except that the riser equations include terms for evaporation from the shell. The control volume mass conservation equations for the riser and downcomer are:

$$\frac{dm_{ri}}{dt} = \dot{m}_{ri,in} - \dot{m}_{ri,out} + \dot{m}_{evap} \qquad \text{Riser (38)}$$

$$\frac{dm_{dc}}{dt} = \dot{m}_{dc,in} - \dot{m}_{dc,out} \qquad \text{Downcomer (39)}$$

The control volume energy equations for the riser and downcomer are:

$$\frac{d}{dt}(mu)_{ri} = (\dot{m}hg)_{ri,in} - (\dot{m}hg)_{ri,out} + \dot{m}_{evap}hg_{xf,surf} \qquad \text{Riser (40)}$$
$$+ h_{xf-ri}A_{xf-ri,wet}(T_{xf,surf,wet}-T_{ri}) + h_{sh,surf,dry}A_{sh,dry}(T_{sh,surf,dry}-T_{ri}) - h_{ri-bf}A_{ri-bf}(T_{ri}-T_{bf})$$

$$\frac{d}{dt}(mug)_{dc} = (\dot{m}hg)_{dc,in} - (\dot{m}hg)_{dc,out} + h_{bf-dc}A_{bf-dc}(T_{bf}-T_{dc}) - h_{dc-sd}A_{dc-sd}(T_{dc}-T_{sd,surf}) \qquad \begin{array}{c}\text{Down}\\ \text{comer}\\ \text{(41)}\end{array}$$

The riser and downcomer energy equations produce no unique pi groups, all have already been derived for the external film, dry shell, baffle, and shield.

Because the air flow develops on a short time scale compared to the vessel time constant, the steady-state form of the momentum equation derived in Appendix A is used for the riser and downcomer. The momentum equation is most useful when applied to a closed path through the downcomer, the riser, the chimney, and the ambient air. The resulting equation is:

$$\left[\right]^{a,c} \tag{42}$$

Equation (42) can be solved with the equations of state, continuity, and the following reasonable distribution assumptions:

- The heat input to the downcomer and riser causes the temperature of each to increase linearly from the inlet to outlet

- The evaporation to the riser causes the mass flow rate and molecular weight to increase linearly from the inlet to outlet

- Temperature and composition are constant over the chimney

With an initial guess of the mass flow rate of air, the evaporated mass of steam, and the temperatures at the downcomer outlet and chimney, Equation (42) can be solved for the air flow rate and the evaporation rate and temperatures calculated. By iteration between the mass, momentum, and energy equations, a solution can be achieved. This process is described in Appendix C, with examples. Alternatively, the equations can be set up and solved by matrix inversion.

The terms in Equation (42) can be made nondimensional by dividing by the sum of the terms on the left side of the equal sign, which is the total system form, friction, and acceleration loss with a value of $\left[\right]^{a,c}$ (The value $\left[\right]^{a,c}$ is somewhat higher than the combined form and friction losses

measured on a model of the PCS air flow path.) The terms on the right side of the equal sign give the following three pi groups:

Downcomer buoyancy   Riser buoyancy   Chimney buoyancy

$$\left[\quad \right]^{a,c} \quad (43) \qquad \left[\quad \right]^{a,c} \quad (44) \qquad \left[\quad \right]^{a,c} \quad (45)$$

4.5 Internal Liquid-Structure Control Volumes

Heat and mass transfer calculations to the internal structures can be simplified by neglecting the heat capacity and thermal resistance of the liquid film. The justification for this simplification follows.

An equation linking the structure to the gas atmosphere through the liquid film can be developed by adding the film Equation (21) and structure Equation (25) for each structure, i, to give:

$$\frac{d}{dt}[(mc_vT)_{st,i} + (mc_vT)_{lf,i}] = (\dot{m}hf)_{lf,in,i} + (\dot{m}_{cond}hg)_{st-ct,i} - (\dot{m}hf)_{lf,out,i} + hA_{st-ct,i}(T_{ct}-T_{lf}) \qquad (46)$$

The structure volumes and surface areas in Table 4-4 and the approximation that the maximum film thickness is 0.005 in. or less permits calculating the ratio of film to structure time constants. The result is a ratio of 0.04 for the steel group with a thickness less than 0.015 ft., 0.015 for the steel with a thickness from 0.015 to 0.051 ft., and less for the others. Consequently, the film time constant is negligible relative to the structure. Reference 7 presented the case that the liquid film heat transfer coefficient is large, so for a scaling analysis it is sufficiently accurate to approximate $T_{st} = T_{lf}$. Thus, Equation (46) can be approximated by:

$$\frac{d}{dt}(mc_vT)_{st,i} = (\dot{m}hf)_{lf,in,i} + (\dot{m}_{cond}hg)_{st-ct,i} - (\dot{m}hf)_{lf,out,i} + hA_{st-ct,i}(T_{ct}-T_{st,i}) \qquad (47)$$

Considering that the film time constant is negligible and the film inflow is zero (condensation is the only source), the liquid film outflow can be set equal to the condensation rate. Using this substitution, Equation (47) reduces to:

$$\frac{d}{dt}(mc_vT)_{st,i} = \dot{m}_{cond}(hg_{ct}-hf_{st,i}) + h_{st-ct,i}A_{st-ct,i}(T_{ct}-T_{st,i}) \qquad (48)$$

Equation (48) shows that while a quantity of heat represented by hg - hf is deposited in the structure, the quantity hg is removed from the atmosphere. The difference, hf, is added to the containment liquid inventory by a negligible volume of liquid.

4.6 Interface Equations

Interface equations are needed to couple adjacent control volumes (in some cases). The interfaces requiring additional equations are containment-liquid film, liquid film-shell, shell-external film, and external film-riser/baffle. The following equations define those interfaces:

$$\dot{m}_{cond} hg_{ct,atm} + h_{ct-lf} A_{ct-lf} (T_{ct} - T_{lf,surf}) = k_{lf} A_{ct-lf} \left. \frac{dT_{lf}}{dx} \right|_{surf} \qquad \text{ct-lf (49)}$$

$$k_{lf} A_{lf-sh} \left. \frac{dT_{lf}}{dx} \right|_{surf} = -k_{sh} A_{lf-sh} \left. \frac{dT_{sh}}{dx} \right|_{surf} \qquad \text{lf-sh (50)}$$

$$k_{sh} A_{sh-xf} \left. \frac{dT_{sh}}{dx} \right|_{surf} = k_{xf} A_{sh-xf} \left. \frac{dT_{lf}}{dx} \right|_{surf} \qquad \text{sh-xf (51)}$$

For the wet portion of the containment outer surface:

$$k_{xf} A_{xf-ri} \left. \frac{dT_{xf}}{dx} \right|_{surf} = \sigma \varepsilon_{xf-ri} A_{xf-ri} (T_{xf,surf}^4 - T_{bf}^4) + h_{xf-ri} A_{xf-ri} (T_{xf,surf} - T_{ri}) + \dot{m}_{evap} hg_{xf,surf} \qquad \text{xf-ri (52)}$$

and for the dry portion of the containment outer surface:

$$k_{sh} A_{sh-ri} \left. \frac{dT_{sh}}{dx} \right|_{surf} = \sigma \varepsilon_{sh-ri} A_{sh-ri} (T_{sh,surf,dry}^4 - T_{bf}^4) + h_{sh-ri} A_{sh-ri} (T_{sh,surf,dry} - T_{ri}) \qquad \text{dry shell (53)}$$

Mass continuity relationships for the subcooled-to-evaporating film, and the downcomer-to-riser interfaces are:

$$\dot{m}_{sc,out} = \dot{m}_{xf,in} \qquad \dot{m}_{ri,in} = \dot{m}_{dc,out} \tag{54}$$

The relationship between the inlet, outlet, and average temperatures of the internal film, external film, riser, and downcomer are necessary to complete the scaling model. The riser and downcomer temperatures are assumed [   ]^{a,c} The internal film is assumed [   ]^{a,c} The external film on AP600 is supplied from a cool source at $T_{sc,in}$ and is assumed [   ]^{a,c}

[   ]^{a,c} The subcooled surface area is determined from Equation (22). The temperature relationships expressing these assumptions are:

$$\left[\qquad\qquad\qquad\qquad\qquad\qquad\qquad\qquad \right]^{(a,c)} \tag{55}$$
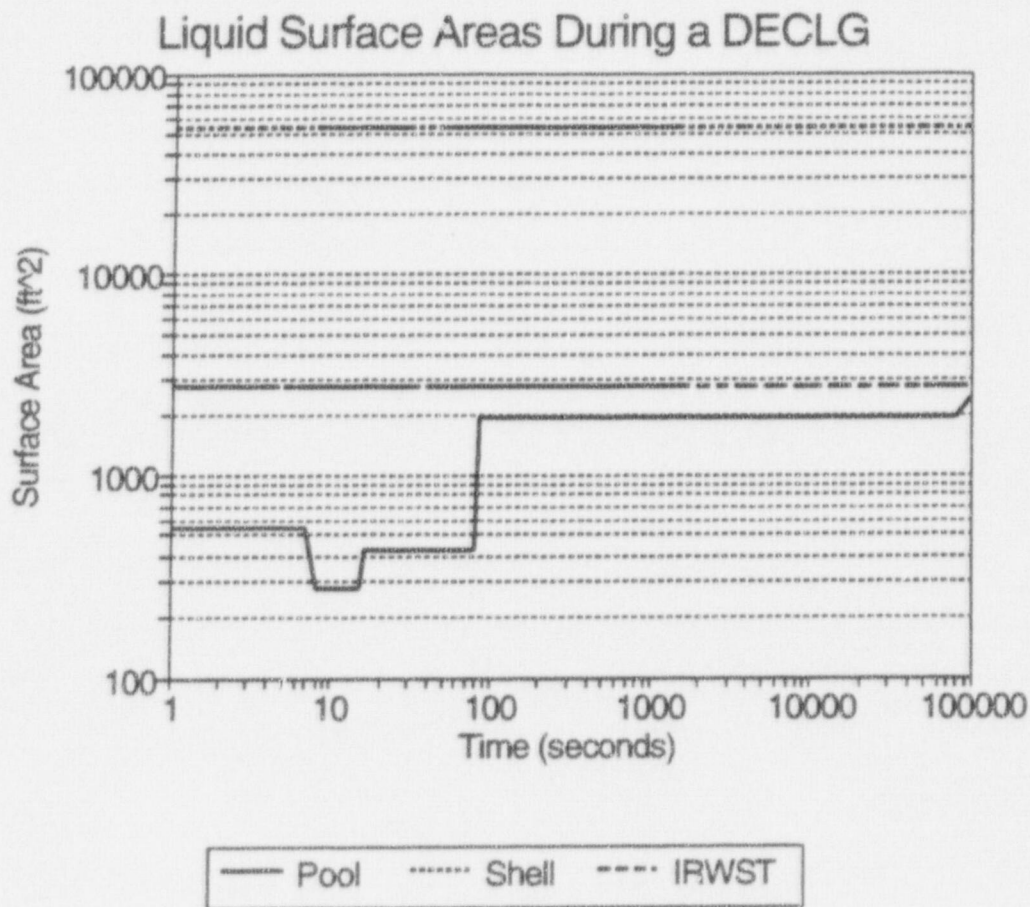
Figure 4-1 Liquid Surface Areas during a DECLG Break
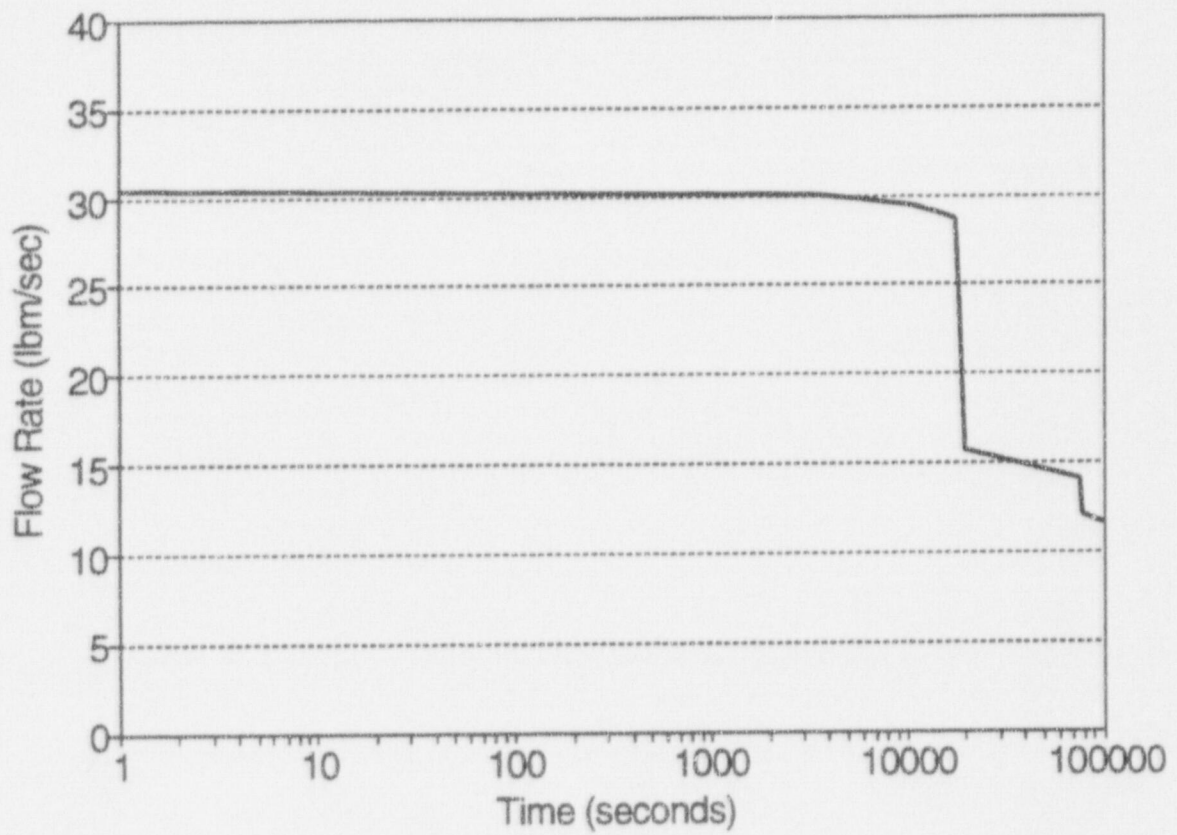
Figure 4-2 External Cooling Water Flow Rate

5.0 CLOSURE RELATIONSHIPS

Time constants and dimensionless groups for the equations presented in Section 4.0 can be developed and evaluated with appropriate closure relationships and assumptions. The relationships and assumptions are presented in the following sections.

5.1 Density and Pressure Relationships Inside Containment

Calculation of the heat transfer and mass transfer to the individual liquid film inside containment requires information on the steam and air density and partial pressure in the bulk containment gas and on each of the individual structure liquid film surfaces. To that end, the following assumptions permit the calculation of the partial density and pressure of steam and air where required.

- The entire inside of the AP600 containment is well mixed, with the exception of jets and boundary layers, by virtue of strong entrainment and ventilation of all below-deck compartments and, therefore, may be represented by a single volume.

- Air and steam are ideal gasses.

- The density of air in containment is equal to the initial density. The partial pressure of air in containment is given by the initial air density and the transient containment temperature history, T_{ct}, from Figure 2-1. The initial containment air composition is assumed to be saturated at 120°F. The partial pressure of steam in containment is the total pressure from Figure 2-1 minus the air partial pressure. The density of steam in containment is calculated from the steam partial pressure, and the density of air in containment is calculated from the air partial pressure. The bulk containment density is the sum of the initial air density plus the steam density.

$$\rho_{ct,air} = 0.06058 \text{ lbm/ft}^3 \quad P_{ct,air} = \frac{\rho_{ct,air}\bar{R}T_{ct}}{M_{air}}$$

$$P_{ct,stm} = P_{total} - P_{ct,air} \quad \rho_{ct,stm} = \frac{P_{ct,stm}M_{stm}}{\bar{R}T_{ct}} \quad \rho_{ct} = \rho_{ct,stm} + \rho_{ct,air} \tag{56}$$

- The break supplies steam and water at a saturation pressure equal to the pressure of containment from Figure 2-1.

- The steam partial pressure and density at the liquid film surface are assumed to be saturated. Thus, the partial pressures and densities at the liquid film surface are calculated:

$$P_{lf,stm} = P_{lf,sat} \qquad \rho_{lf,stm} = \frac{P_{lf,stm} M_{stm}}{R T_{lf}}$$

$$P_{lf,air} = P_{tot} - P_{lf,stm} \qquad \rho_{lf,air} = \frac{P_{lf,air} M_{air}}{R T_{lf}} \qquad \rho_{lf} = \rho_{lf,air} + \rho_{lf,stm}$$

(57)

- The boundary layer density and temperature are assumed to be the average of the containment and liquid film surface values. The dynamic viscosity and thermal conductivity are the average of the bulk and surface mixture values. The bulk and surface mixture values are the respective mole fraction-weighted averages in the bulk and at the surface.

These properties permit the evaluation of all mass and energy fluxes required to calculate the pi groups.

5.2 Heat and Mass Transfer Relationships

The heat and mass transfer relationships used for the scaling analysis are the same correlations developed for use on AP600 in the WGOTHIC code, with the exception that in the scaling model, only free convection is used inside containment. Validation of these relationships using separate effects tests has been documented and presented[8,9]. A summary of the heat and mass transfer relationships used in the scaling analysis follows.

The inside of containment operates under free convection, except for the first few seconds of the blowdown. Thus, the use of free-convection correlations on the inside is expected to underpredict heat and mass transfer during blowdown, and is expected to be accurate thereafter. The free convection mass transfer coefficient is given by the McAdams correlation for vertical surfaces and was extended to inclined surfaces by the work of Vliet:[10]

$$Nu_{free} = 0.13 \, Gr_H^{1/3} Pr^{1/3}$$

(58)

The riser operates with forced-convection heat transfer for all times of interest in the scaling analysis. The Colburn forced-convection heat transfer equation for channels is used for the riser:

$$Nu_{forced} = 0.023 \, Re_D^{4/5} Pr^{1/3}$$

(59)

where the Nusselt number and Reynolds numbers are based on the channel hydraulic diameter.

The downcomer operates with mixed, free, and forced convection. For mixed convection, Equations (58) and (59), with Nusselt, Reynolds and Grashof numbers based on channel diameter, are combined as recommended by Churchill.[11] For opposed free and forced convection, as occurs in the downcomer, the mixed convection correlation is:

$$Nu_{mixed} = (Nu_{free}^3 + Nu_{forced}^3)^{1/3} \tag{60}$$

The heat and mass transfer analogy is used to get a mass transfer coefficient from either the free-, forced-, or mixed-convection heat transfer coefficient:

$$Sh = Nu \left(\frac{Sc}{Pr} \right)^{1/3} \tag{61}$$

The dimensionless Sherwood number, defined in Section 12.0, provides the necessary correction to the mass transfer coefficient for high mass transfer rates. The corresponding correction to the heat transfer coefficient for high mass transfer rates is neglected since heat transfer is always negligible whenever there is mass transfer.

The resulting expressions for the heat and mass transfer coefficients are:

$$h_{free} = (0.13) \frac{k \, Pr^{1/3}}{(v^2/g)^{1/3}} \left(\frac{2(\rho_{surf} - \rho_{ct})}{\rho_{surf} + \rho_{ct}} \right)^{1/3} \tag{62}$$

$$h_{force} = 0.023 \frac{k}{d_h} Pr^{1/3} \left(\frac{v \, d_h}{v} \right)^{4/5} \tag{63}$$

$$k_g = \frac{h \, D_v \, P}{RT \, p_{Bm} \, k} \left(\frac{Sc}{Pr} \right)^{1/3} \tag{64}$$

When the structure temperatures begin to reduce due to containment cool down, the structures become heat sources. However, their heat transfer coefficients no longer include mass transfer because the surface is hotter than the ambient. With only convective heat transfer, the total heat transfer rate from internal structures decreases by 1 to 2 orders of magnitude, greatly reducing their importance as a heat source.

6.0 ANALYTICAL SCALING MODEL FOR AP600

The primary goals of this scaling analysis are:

- Calculate the pi groups for AP600, thereby demonstrating the dominant phenomena responsible for pressurizing the AP600 containment during a DECLG

- Relate the large-scale tests (LST) to AP600 to determine their validity as an experimental basis to support AP600

The preceding sections presented the development of a large number of equations necessary to scale AP600. The equations embody the important phenomena identified in the PIRT. Those equations were solved to produce a pressure history for AP600, and the scaling model was validated by comparing predictions with measurements from the LST. The validation of the scaling model supports the completeness of the PIRT. [A transient scaling model and a steady-state scaling model were developed. The transient scaling model predicts behavior out to approximately 10,000 seconds, and the steady-state scaling model was used to predict the steady-state interactions with the air flow path at 660, 2000, 4000, and 8000 seconds.

6.1 Transient Model

The transient scaling model was run for the first 10,000 seconds of the transient. The model made use of the knowledge that the containment pressure is only weakly coupled to the air annulus until after the external film flow is established (assumed to be at 11 minutes). After 11 minutes, it was assumed that the external flow rate was 30 lbm/sec and that all of the water evaporated[5,6] for the 10,000 seconds modeled. Thus, although the external conditions are not explicitly calculated in the transient scaling model, the major effect of coupling to the outside is known. The LSTs consistently showed that the water evaporation rate is approximately the same as the the steam flow rate minus the subcooled heat. Regardless of the shell temperature, the containment can reject little more heat than results from evaporating the entire inventory of external water. The calculations showed that the shell temperature predicted by this scaling model was sufficient to evaporate all the water over less than half the surface area, and the stability model[5,6] showed that the film would cover sufficient area to fully evaporate. Figure 6-1 shows a comparison of the transient scaling model pressure comparison to that of WGOTHIC for the DECLG.

6.2 Steady-State Scaling Model

A steady-state scaling model of AP600 was constructed using the steady-state form of the control volume equations presented in Appendix A. The scaling model coupled the outside of containment to the inside and was constructed for the purpose of examining pi groups outside containment. This scaling model was used to predict the heat and mass flows and fluxes in both AP600 and in a LST at similar internal temperatures and pressures. The use of this scaling model on AP600 required

specification of the containment pressure and temperature. Values were taken from Figure 2-1, although values predicted by the scaling model would have produced nearly identical results.

Application of the scaling model to the LST permitted the validity of the steady-state scaling model to be assessed. The steady-state scaling model calculated total vessel heat removal within 5 percent of the measurements from the LSTs used to benchmark the steady-state calculations at 2000, 4000, and 8000 seconds. This level of agreement indicates that the important phenomena identified in the PIRT for AP600 are sufficient to accurately predict performance. Therefore, a model that includes those phenomena and phenomenological models can be applied to AP600.

6.3 Limits of Analytical Scaling Model

The concentration distribution of noncondensables (air) in the containment atmosphere was determined to have a significant effect on the steady-state pressure. The containment atmosphere stratifies with the air concentration lowest in the dome and increasing at lower elevations. The effect is to enhance mass transfer rates in the upper containment due to the strong dependence of the mass transfer rate on noncondensables and steam partial pressure. The lower part of containment, where air concentrations are higher, is below deck and not exposed to the wetted shell; so the $\qquad$]a,c

[$\qquad$]a,c

It was determined from the scaling calculations discussed in Sections 7 and 8 that by specifying the internal distribution of noncondensables, the scaling model produced pressure and total heat rejection nearly identical to the values measured in the LST. This comparison demonstrates that the mass transfer model is a good model. The scaling analysis in Section 7 shows that mass transfer is the primary mode of heat rejection from containment to the atmosphere.

An internal phenomena that has not been included in the scaling model is detailed treatment of the jet. The Froude number evaluations and comparisons presented in Sections 7 and 8 show that the quasi-steady, post-wetting phase of the DECLG transient in AP600 is characterized by a steam source with negligible kinetic energy. All of the LST performed with the diffuser and with the diffuser under the steam generator are good simulations of AP600. The LST with the 3-in. steam source[a,c

[$\qquad$]a,c

The conclusions that can be drawn from the comparisons are:
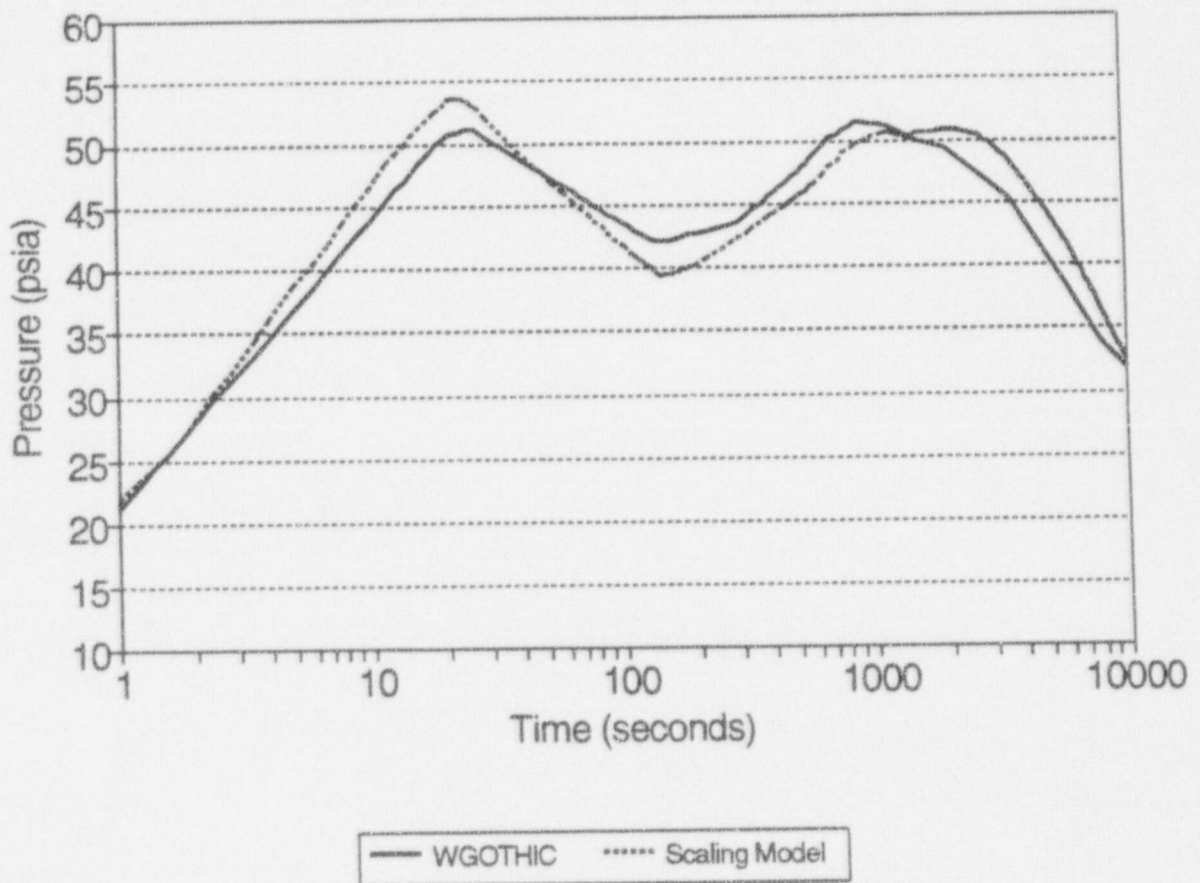
[$\qquad$]a,c

a,c

Figure 6-1 Scaling Model Pressure History Comparison to WGOTHIC Prediction

7.0 CALCULATED RESULTS FOR AP600

The DECLG transient is driven by a mass and energy source, the magnitude of which changes by several orders of magnitude from early to late in the transient. Consequently, transport phenomena that are not very important during blowdown become dominant late in the transient. As a result, nondimensionalizing transport processes based on initial conditions obscure the relationships between transport processes later in the transient. Thus, the time history of the pi groups was calculated by dividing flux values by the instantaneous source flux.

7.1 Containment Scaling Relationships

The time constants and pi groups for the AP600 containment were calculated using the transient scaling model out to 10,000 seconds and are presented in Table 7-1. The internal heat sinks, the pool, and the containment shell are represented. Heat and mass transfer from the containment atmosphere to the IRWST is even less than for the pool and was not included. All internal heat sinks (steel and concrete) were combined and are represented by one pi group. The shell heat removal was divided into subcooled, wetted, and dry fractions with a pi group for each. The convection heat transfer for all structures and the pool was combined in one pi group.

The scaling groups show that heat transfer is insignificant in comparison to mass transfer, and that the internal heat sinks have a major effect until several thousand seconds into the transient. The values of the pool condensation group, Π_{pool}, suggest that late in the transient, the pool evaporation becomes an additional source of steam that should not be neglected.

The Froude number for the steam source in containment can be examined to provide insight into internal mixing processes. The Froude number used here is the ratio of the steam source kinetic energy, $\rho_{jet}v^2$, to the potential energy of the jet in containment, $(\rho_{amb}-\rho_{jet})gH$. The Froude number peaks at 1200 at the start of blowdown and has a peak value of 0.28 during post-blowdown. At 2000 seconds, the Froude number is 0.003, and decreases thereafter. Clearly, the post-blowdown kinetic energy of the jet is much too low to produce significant velocities inside containment. The values of the Froude number support the claim that the containment is well-mixed during blowdown because of the relatively high kinetic energy jet (Fr = 1200). During post-blowdown, the Froude numbers indicate the jet kinetic energy is too low to mix (Fr < 0.3), although the buoyant plume still does induce good mixing. These Froude numbers also provide a basis for comparison to the LST in Section 8.0. The jet source is considered to be the flow area out of the steam generator compartment into the above-deck volume.

TABLE 7-1
AP600 INTERNAL CONTAINMENT TIME CONSTANTS
AND PI GROUPS FROM TRANSIENT SOLUTION

	Time into Transient (seconds)									a,c
	5	20	100	500	1000	2000	4000	8,000	10,000	
τ_{ct}										
$\Pi_{\text{internal heat sinks}}$										
$\Pi_{\text{evaporating shell}}$										
$\Pi_{\text{subcooled shell}}$										
$\Pi_{\text{dry shell}}$										
Π_{pool}										
$\Pi_{\text{all convection ht}}$										
Π_{press}										

7.2 Air Flow Path Heat Transfer Scaling Relationships

Transient processes outside containment are not important to containment pressure a few hundred
seconds after the initial external film wetting. After that, any temperature or flow changes outside
containment are slow enough to be considered quasi-steady. Consequently, a system of steady- state
equations can be solved to determine the magnitude of transport processes and to evaluate the
pi groups. The system of steady-state equations solved for AP600 is presented in Appendix A. The
values of the pi groups are presented in Table 7-2. The scaling groups were developed in Section 4.0,
and all are ratios of energy flux terms divided by the steam source term.

One additional dimensionless group can be defined for the riser to represent the sensible heat input
from the evaporated water. The vapor is assumed to leave the liquid film at the film surface
temperature and exits the riser at the riser outlet temperature. This group is needed to permit
comparisons between the riser and downcomer total sensible heat inputs. The group is:

$$\left[\right]^{a,c}$$

(65)

Shell	**Dry 660 sec**	**2000 sec**	**4000 sec**	**8000 sec**	**Baffle**	**Dry 660 sec**	**2000 sec**	**4000 sec**	**8000 sec**

TABLE 7-2
AP600 EXTERNAL PI GROUPS

The shell pi groups in Table 7-2 account for all of the shell heat losses, but do not add up to 1.000 because the internal heat sinks and atmosphere are either absorbing or releasing significant quantities of energy relative to the source. At 660 seconds, nearly all of the source is being stored internally. At 2000 seconds, the steam source is greater than the shell evaporation, but 20 percent of the source energy is being stored in internal heat sinks (primarily the concrete), which accounts for the decreasing containment temperature and pressure. At 4000 seconds, the shell evaporation rate exceeds the source energy rate, but the internal storage still is absorbing 19 percent of the source. At 8000 seconds, energy storage in internal heat sinks (again, the concrete) has reduced to 6 percent. The atmosphere, which at the peak pressure contains approximately 200,000 lbm of steam, represents an enormous source of stored energy and is responsible for the net excess of outflow over inflow.

The ex-containment scaling groups show that for the wet containment, evaporation is the major heat removal mechanism, and that heat transfer to the subcooled external liquid film and convective heat transfer are both second order. Radiation heat transfer from containment is approximately half that of convection or subcooling.

The ratio of downcomer to riser sensible heats shows that the downcomer receives only 27 to 37 percent of the sensible heat input to the riser. The potential effect of fog[7] in the riser is to reduce the radiation heat transfer to the baffle and further reduce both the heat input to the downcomer and the ratio of downcomer-to-riser heat input. These ratios suggest that any potential effect associated with heat input to the downcomer is significantly smaller than in the riser. Further information on the minor role of the downcomer is provided by the momentum comparisons in Section 7.3.

7.3 Air Flow Path Momentum Scaling

The momentum scaling groups for the air flow path were derived in Section 4.4 and are presented in Table 7-3 for a dry exterior just prior to the initial application of water at 660 seconds, and for wet exterior conditions at 2000, 4000, and 8000 seconds. The values in Table 7-3 represent the fraction of the total buoyancy induced pressure drop around the air flow path; the three values sum to 1.000. The negative values for the riser indicate buoyant pressure acting counter to the direction of flow.

TABLE 7-3 AP600 AIR FLOW PATH MOMENTUM SCALING TERMS				
Scale Group	Dry, 660 sec	Wet, 2000 sec	Wet, 4000 sec	Wet, 8000 sec
$\Pi_{downcomer}$				
Π_{riser}				
$\Pi_{chimney}$				

a,c

The scaled buoyancy terms show that the effect of heat transfer to the downcomer, as it affects momentum, is a small negative part of the total buoyancy-induced driving pressure. The calculations of the buoyant pressure in the riser and chimney at 2000 seconds showed the buoyancy is 35 percent due to molecular weight and 65 percent due to temperature rise. The downcomer clearly has a minor effect on the air flow in the downcomer-riser-chimney flow path.

8.0 SCALING OF LST

The important scaling groups for AP600 were determined to be those for condensation inside containment, and evaporation and subcooled heat transfer outside containment. Because heat transfer through the shell is one-dimensional, the steady-state heat and mass transfer on the inside of containment must match the distribution on the outside. Consequently, it is sufficient to consider only the two external scaling groups for subcooled heat transfer and for evaporation. The scaling group values were determined from measurements for three large-scale tests (218.1B, 217.1A, and 222.1) and are presented in Table 8-1. The tests selected had internal temperatures and pressures similar to those expected for AP600 at the selected comparison times. The ratio of the large-scale test (LST) to AP600 pi groups, $\Pi^R = \Pi_{AP600}/\Pi_{LST,meas}$, are presented in Table 8-1. The AP600 values were taken from Table 7-2, and were renormalized to the fraction of the source energy that escapes through the shell (subcooling, evaporation, radiation, and convection). In the LST, all of the source escapes through the shell, while in AP600 a portion is either deposited in or released from the internal heat sinks and atmosphere. The ratios show that the LSTs selected for comparisons had approximately four times the scaled subcooled heat removal of AP600, while the evaporative mass transfer energy is 90 percent of that in AP600.

TABLE 8-1 LARGE-SCALE TEST PI GROUPS SCALED TO AP600							
Large-Scale Test				**AP600 Simulation Time**			
PI Group	218.1B	217.1A	222.1	PI Group	2000 sec	4000 sec	8000 sec
Π_{evap}				Π_{evap}			a,c
$\Pi_{subcooled}$				$\Pi_{subcooled}$			
Scaled Ratio: LST/AP600							
	PI Ratio	218.1B 2000 sec	217.1A 4000 sec	222.1 8000 sec			
	Π^R_{evap}				a,c		
	$\Pi^R_{subcooled}$						

The comparisons in Table 8-1 show that the evaporative heat transfer in the LST is very close to AP600 while the subcooled comparison is less satisfactory. The extra subcooling in the LST is due to two factors in the tests: the scaled external water flow rate is approximately two times too high, and the source temperature is much less than the 120°F assumed for safety reasons for AP600. In reality, the AP600 source temperature will always be less than 120°F, resulting in real subcooled values approximately twice those presented in Sections 7.0 and 8.0.

The LST were conducted with three different steam source configurations: a 3-in. diameter pipe, an 18-in. diameter diffuser, and the diffuser located in a simulated steam generator compartment. Froude numbers calculated for the tests revealed that values greater than 200 produced a well-mixed containment. Such high Froude numbers are similar to the AP600 blowdown values and support the expectation of well-mixed containment during blowdown. The LST conducted with the simulated steam generator produced steady-state Froude numbers that ranged from 0.0002 to 0.02. From these values it is concluded that the LST with the steam generator are the appropriate tests to compare to the post-blowdown AP600 (Fr = 0.003 at 2000 seconds). This guidance was followed in the selection of the LST tests compared to AP600 in this section. The range of steady-state numbers achieved in the LST 0.0002<Fr<0.02 spans the Froude number range in AP600 0.0008Fr<0.003 from 2000 to 8000 sec.

Heat and mass transfer predictions were made with the scaling model for the three representative large scale tests noted previously. The calculation is described in Appendix C. The scaling model predicted 81, 70, and 97 percent of the measured test heat removal. When the measured noncondensable distributions were input directly into the model, rather than using the well-mixed assumption built into the model, the predicted heat removals were 96, 98 and 97 percent of the measured values. These comparisons demonstrate that the accuracy of the well-mixed model depends upon how closely the measured noncondensable distributions compare to the well-mixed values.

Given the measured concentrations, the scaling model shows that it can consistently achieve a high level of agreement with the measurements. This is because condensation and evaporation are the dominant energy transport mechanisms, and the selected correlations are appropriate. Because this clearly emphasizes the importance of the phenomenological relationships for mass transfer, work is underway to perform a more complete comparison between the mass transfer correlations and all relevant large scale tests.

9.0 NONPROTOTYPICAL TEST CHARACTERISTICS

The scaled relationships show that there are only two significant nonprototypic characteristics in the large-scale test (LST) that caused the results to deviate from the expected AP600 behavior. Both of these nonprototypicalities are understood and can be accommodated analytically in the scaling modeling.

a,c

10.0 CONCLUSIONS

The major results and conclusions of this scaling analysis are:

- All phenomena have been identified and ranked in a phenomena identification and ranking table (PIRT).

- Control volume equations and closure relationships were developed for the significant phenomena and integrated into a scaling model that coupled the inside of containment to the external PCS.

- Comparison of the scaling model predictions to large-scale test results validated the completeness of the PIRT and the scaling model equations.

- The selected phenomenological models are dimensionless, scalable, and valid for application to both the large-scale tests and AP600.

a,c

11.0 REFERENCES

1. "AP600 Standard Safety Analysis Report", Westinghouse Electric Corporation, June 26, 1992.

2. NUREG/CR-5809 EGG-2659, "An Integrated Structure and Scaling Methodology for Severe Accident Technical Issue Resolution," INEL, EG&G Idaho, Inc.

3. Letter, N. J. Liparulo (Westinghouse) to R. W. Borchardt (US NRC), "AP600 Passive Containment Cooling System Preliminary Scaling Report", NTD-NRC-94-4246, DCP/NRC0171, Docket No.: STN-52-003, July 28, 1994.

4. Letter, N. J. Liparulo (Westinghouse) to R. W. Borchardt (U.S.NRC), "AP600 PCS Design Basis Analysis Models and Margin Assessment Report", NTD-NRC-94-4174, DCP/NRC0111, Docket No.: STN-52-003, June 30, 1994.

5. Letter, N. J. Liparulo (Westinghouse) to R. W. Borchardt (U.S. NRC), "AP600 Passive Containment Cooling System Letter Reports" (Method for Determining Film Flow Coverage for the AP600 Passive Containment Cooling System), NTD-NRC-94-4247, DCP/NRC0172, Docket No.: STN-52-003, July 28, 1994.

6. Letter, N. J. Liparulo (Westinghouse) to R. W. Borchardt (US NRC), "Supplemental Information on AP600 PCS Film Flow Coverage Methodology," NTD-NRC-94-4286, August 31, 1994.

7. NTD-NRC-94-4100 (Docket No. STN-52-003) Letter, N. J. Liparulo (Westinghouse) to R. W. Borchardt (NRC), "AP600 Passive Containment Cooling System Letter Reports, "Radiation Heat Transfer through Fog in the Passive Containment Cooling System Air Gap", and "Liquid Film Model Validation".

8. Letter, N. J. Liparulo (Westinghouse) to R. W. Borchardt (U.S. NRC), Presentation Materials from the March 17, 1994 Meeting on AP600 Passive Containment Cooling System Design Basis Analysis, NTD-NRC-94-4083, March 21, 1994.

9. Letter, N. J. Liparulo (Westinghouse) to R. W. Borchardt (US NRC), "Experimental Basis for Convective Heat Transfer Selected for Modeling Heat Transfer from AP600 Containment Vessel", NTD-NRC-94-4287, August 31, 1994.

10. G. C. Vliet, "Natural Convection Local Heat Transfer on Constant-Heat Flux Inclined Surfaces," *Journal of Heat Transfer*, November, 1969, pp. 511-516.

11. S. W. Churchill, "Combined free and Forced Convection Around Immersed Bodies", Section 2.5.9, and "Combined Free and Forced Convection in Channels", Section 2.5.10 in E. U . Schlunder, Ed.-in-Chief, *Heat Exchanger Design Handbook*, Hemisphere Publishing Corp. 1983.

12.0 NOMENCLATURE

Symbol   Quantity

Letters

A	Area
c_p	Constant pressure specific heat
c_v	Constant volume specific heat
d	Hydraulic diameter
D_v	Gas phase diffusion coefficient
g	Gravitational acceleration
h	Convective heat transfer coefficient
hg	Gas phase enthalpy
hf	Liquid phase enthalpy
hfg	Liquid-to-gas enthalpy
H	Height
k	Thermal conductivity
k_g	Gas phase mass transfer coefficient
L	Length
m	Mass
$\dot{m}$	Mass flow rate
P	Pressure or partial pressure
P_{Bm}	Log mean pressure difference = $(P_2-P_1)/\ln(P_2/P_1)$
$\dot{q}$	Heat flow rate
Q	Volumetric flow rate
$\overline{R}$	Universal gas constant
T	Temperature
uf	Liquid phase internal energy
ug	Gas phase internal energy
ufg	Liquid-to-gas internal energy
V	Volume

Subscripts

air	Air
bf	Baffle
cc	Concrete
ch	Chimney
cond	Condensate
ct	Containment gas
dc	Downcomer

evap	Evaporation
h	Heat transfer
in	Inlet value
k	Mass transfer
lf	Liquid film
out	Outlet value
pl	Pool
ri	Riser
rw	IRWST water
sc	Subcooled external liquid film
sd	Shield building
sh	Containment shell
sat	Saturated
st	Structure
stm	Steam
wat	Water
xx-yy	Value at the interface between xx and yy
0	Initial or boundary value for nondimensionalizing

Superscripts

+	Nondimensional value
R	Ratio of LST to AP600 Pi groups

Greek Letters

δ	Structure or liquid film thickness
ρ	Density
ν	Kinematic viscosity
τ	Time constant

Dimensionless Groups

Gr	Grashof number = $g(\rho_2-\rho_1)L^3/\rho_1\nu^2$
Nu	Nusselt number = hL/k
Pr	Prandtl number = $\mu c_p/k$
Sc	Schmidt number = $\mu/\rho D_v$
Sh	Sherwood number = $k_g RT P_{Bm} L/D_v P$
Π	Dimensionless Scaling Group

APPENDIX A
CONTROL VOLUME EQUATIONS AND DERIVATION OF SCALE GROUPS

CONTROL VOLUME EQUATIONS AND DERIVATION OF SCALE GROUPS

The control volume equations for mass, momentum, and energy are derived in many introductory fluid dynamics textbooks. Shames[1], Shapiro[2], Hughes and Brighton[3], and Bird, Stewart, and Lightfoot.[4] present the development with helpful information on control volumes. Additional information is provided in NUREG/CR-5809[5]. The following example will illustrate how the control volume equations are developed and made nondimensional for a control volume around the containment gas.

Conservation of Mass

Conservation of mass for a control volume can be stated as: "the net afflux rate of mass through the control surface equals the rate of decrease of mass inside the control volume." The mass conservation equation applies to the liquid and gas control volumes. These are the containment gas, the internal containment liquid film, the external containment liquid film, the riser, and downcomer. The following equation is used for conservation of mass in a control volume:

$$\frac{d}{dt}\int_{vol}\rho\,dV = \int_{surf}\rho\,\bar{v}\cdot d\bar{A}$$

(1)

with the sign convention that fluxes into the control volume are positive. If density and velocity can be represented by average values, the equation for conservation of mass in a control volume can be written:

$$\sum_{i=1}^{n}(\rho_i v_i A_i) = \frac{d}{dt}(\rho V) \quad \text{or in terms of mass:} \quad \sum_{i=1}^{n}\dot{m}_i = \frac{dm}{dt}$$

(2)

Containment Gas Volume Example:

Terms are required to represent the steam break source and pool evaporation into containment and the mass condensed on the solid surfaces and IRWST. Using the nomenclature of the scaling report:

$$\frac{dm_{ct,stm}}{dt} = \dot{m}_{stm,in} - \sum_{i=1}^{6}\dot{m}_{ct-lf,i} + \dot{m}_{ct-pl} - \dot{m}_{ct-rw}$$

$$\text{and} \quad \frac{dm_{ct,air}}{dt} = 0$$

(3)

Equation 3 can be made nondimensional with the following substitutions:

$$m = m_0 m^+$$
$$\dot{m} = \dot{m}_0 \dot{m}^+$$

The resulting dimensionless equation for steam conservation is:

$$m_0 \frac{dm^+}{dt} = \dot{m}_{stm,in,0} \dot{m}^+_{stm,in} - \sum_{i=1}^{6} \dot{m}_{ct-lf,i,0} \dot{m}^+_{ct-lf,i} + \dot{m}_{pl-ct,0} \dot{m}^+_{pl-ct} - \dot{m}_{ct-rw,0} \dot{m}^+_{ct-rw} \tag{4}$$

Dividing the dimensionless equation by the source term gives:

$$\tau_{ct} \frac{dm^+}{dt} = \dot{m}^+_{stm,in} - \sum_{i=1}^{6} \Pi_{ct-lf,i} \dot{m}^+_{ct-lf,i} + \Pi_{pl-ct} \dot{m}^+_{pl-ct} - \Pi_{ct-rw} \dot{m}^+_{ct-rw} \tag{5}$$

where the time constant is:

$$\tau_{bl} = \frac{m_{ct,stm,0}}{\dot{m}_{stm,in,0}} \tag{6}$$

and the pi groups are:

$$\left[\right]^{a,c} \tag{7}$$

Conservation of Energy

The energy conservation equation is required for the [containment gas, internal liquid film, containment shell, external liquid film, riser, baffle, downcomer, and shield.]^{a,c} Conservation of energy in a control volume is given by:

$$\frac{d}{dt} \int_{vol} e\rho \, dV = \int_{surf} e(\rho \bar{v} \cdot d\bar{A}) + \frac{dq}{dt} - \frac{dW}{dt} \tag{8}$$

The term dq/dt represents the heat transfer across the control surface and can include conduction, convection, and radiation heat transfer. The term dW/dt represents all the work interactions across the control surface. There is no shaft work, so the only work interaction is the flow work:

$$\text{Flow Work} = \int_{\text{surf}} \bar{\bar{\pi}} \cdot \bar{v} \, dA \tag{9}$$

Even though there may be shear stresses at the interfaces between control volumes, there is no shear work unless the velocity at the control surface is non-zero. For example, in pipe flow there is net flow work on the control volume due to the pressure drop along the length of the pipe, but because the velocity is zero at the pipe surface, there is no work term. The shear stress and form losses do appear in the momentum equation and do affect the magnitude of the pressure drop, and thus are indirectly included in the energy equation.

Containment Gas Energy Equation Example:

The control volume equations and scaling groups can be developed for conservation of energy applied to the containment gas control volume similar to the development for the mass equation. The energy equation will include additional terms for convective heat transfer and for pressure. The energy equation for the containment gas is:

$$\left[\qquad\qquad\qquad\qquad \right]^{a,c} \tag{10}$$

Equation 10 can be made nondimensional with the following substitutions:

$$
\begin{aligned}
A &= A_0 \, A^+ \\
h &= h_0 \, h^+ \\
\dot{m} &= \dot{m}_0 \, \dot{m}^+ \\
P_\alpha &= P_{\alpha,0} \, P^+_\alpha \\
T &= T_0 \, T^+ \\
V_\alpha &= V_{\alpha,0} \, V^+_\alpha
\end{aligned}
$$

Substituting these terms into Equation 10, neglecting the volume change term, and dividing by the steam source term gives:

$$\Bigg[\hspace{10cm} \Bigg]^{a,c}$$

(11)

where the time constant is:

$$\tau_{ct} = \frac{m_{ct,stm,0}}{\dot{m}_{stm,in,0}}$$

(12)

the pi groups are:

$$\Bigg[\hspace{10cm} \Bigg]^{a,c}$$

(13)

(14)

(15)

and the dimensionless temperature is:

$$\theta_T = \frac{(T_{ct,0} - T_{lf,surf,i,0})}{T_{ct,0}}$$

(16)

Conservation of Momentum

The momentum equation can be written for the gas and liquid phases. However, the Nusselt equation as modified by Chun and Seban for wavy laminar films is used for the liquid film momentum. Although this is a steady-state equation, the liquid film heat capacity was determined to be negligible.

The downcomer and riser require a momentum equation to solve for the air flow rate induced by the buoyant force of the heated air and evaporated steam. A useful form of the momentum equation can be derived by [

development proceeds as follows, [$]^{a,c}$ $]^{a,c}$ The

$$[\qquad\qquad]^{a,c} \tag{17}$$

This reduces to:

$$[\qquad\qquad]^{a,c} \tag{18}$$

and when integrated around the closed path through the downcomer, riser, chimney and ambient air to the downcomer inlet is:

$$[\qquad\qquad]^{a,c} \tag{19}$$

By adding the integral of the density of the ambient air around the same closed path, which is equal to zero, Equation 19 becomes:

$$\left[\right]^{a,c} \qquad (20)$$

Steady-State Equations

The following system of equation was solved to determine the heat and mass transfer from the inside of the AP600 containment to the external PCS. At steady state the conservation of mass equations can be written:

$$\dot{m}_{cond} = \dot{m}_{lf,out} \qquad \text{Liquid film (21)}$$

$$\dot{m}_{xf,in} = \dot{m}_{xf,out} + \dot{m}_{evap} \qquad \dot{m}_{sc,out} = \dot{m}_{xf,in} \qquad \text{External film (22)}$$

$$\dot{m}_{ri,air,in} = \dot{m}_{ri,air,out} \qquad \dot{m}_{ri,stm,in} + \dot{m}_{evap} = \dot{m}_{ri,stm,out} \qquad \text{Riser (23)}$$

$$\dot{m}_{dc,air,in} = \dot{m}_{dc,air,out} \qquad \dot{m}_{dc,stm,in} = \dot{m}_{dc,stm,out} \qquad \text{Downcomer (24)}$$

The steady-state mass-energy equations, with the known mass flow rates substituted for the unknown flow rates, and the shield assumed to be at a known temperature, are:

Liquid film (lf) for each structure, i

$$\dot{m}_{cond}[c_{v,wal}(T_{ct}-T_{lf,i,out})+hfg_{ct,stm}] + h_{ct-lf,i}A_{ct-lf,i}(T_{ct}-T_{lf,i,surf}) = \frac{2k_{lf}}{\delta_{lf}}(T_{lf,surf,i}-T_{lf-sh,i}) \qquad \text{Lf (25)}$$

$$\frac{2k_{sh}}{\delta_{sh}}(T_{lf-sh}-T_{sh}) = \frac{2k_{sh}}{\delta_{sh}}(T_{sh}-T_{sh-xf}) \qquad \text{Shell (26)}$$

$$0 = \dot{m}_{xf,in}(hf_{sc,in}-hf_{sc,out}) + \frac{2k_{sc}}{\delta_{sc}}(T_{sh-sc}-T_{sc}) \qquad \begin{array}{l}\text{Subcooled}\\ \text{film (27)}\end{array}$$

$$\dot{m}_{xf,in}c_{v,wat}(T_{xf,in}-T_{xf,out}) - \dot{m}_{evap}[hfg_{xf,surf}+c_{v,wat}(T_{xf,surf}-T_{xf,out})]$$

Evaporating film (28)

$$- h_{xf-ri}A_{xf-ri}(T_{xf,surf}-T_{ri}) - \sigma\varepsilon A_{xf-ri}(T_{xf,surf}^4-T_{bf}^4) = \frac{-2k_{xf}}{\delta_{xf}}(T_{sh-xf}-T_{xf})$$

$$[(\dot{m}_{ri,air,in}c_{p,air}+\dot{m}_{ri,stm,in}c_{p,stm})(T_{ri,in}-T_{ri,out}) + \dot{m}_{evap}c_{p,stm}(T_{xf,surf}-T_{ri,out})$$

Riser (29)

$$+ h_{xf-ri}A_{xf-ri}(T_{xf,surf}-T_{ri}) - h_{ri-bf}A_{ri-bf}(T_{ri}-T_{bf}) = 0$$

$$\sigma\varepsilon_{xf-bf}A_{ri-bf}(T_{xf,surf}^4-T_{bf}^4) - \sigma\varepsilon_{bf-sd}A_{dc-sd}(T_{bf}^4-T_{sd,surf}^4)$$

Baffle (30)

$$+ h_{ri-bf}A_{ri-bf}(T_{ri}-T_{bf}) - h_{bf-dc}A_{bf-dc}(T_{bf}-T_{dc}) = 0$$

$$(\dot{m}_{dc,air,in}c_{p,air}+\dot{m}_{dc,stm,in}c_{p,stm})(T_{dc,in}-T_{dc,out})$$

Downcomer (31)

$$+ h_{bf-dc}A_{bf-dc}(T_{bf}-T_{dc}) + h_{sd-dc}A_{sd-dc}(T_{sd}-T_{dc}) = 0$$

Conservation of energy equations are also required for interfaces

$$\dot{m}_{cond}hg_{ct,stm} + h_{ct-lf}A_{ct-lf}(T_{ct}-T_{lf,surf}) = \frac{2k_{lf}}{\delta_{lf}}A_{ct-lf}(T_{lf,surf}-T_{lf})$$

ct-lf (32)

$$\frac{2k_{lf}}{\delta_{lf}}A_{lf-sh}(T_{lf}-T_{lf-sh}) = \frac{2k_{sh}}{\delta_{sh}}A_{lf-sh}(T_{lf-sh}-T_{sh})$$

lf-sh (33)

$$\frac{2k_{sh}}{\delta_{sh}}A_{sh-xf}(T_{sh}-T_{sh-xf}) = \frac{2k_{xf}}{\delta_{xf}}A_{sh-xf}(T_{sh-xf}-T_{xf})$$

sh-xf (34)

$$\frac{2k_{xf}}{\delta_{xf}}A_{xf-ri}(T_{xf}-T_{xf,surf}) = \sigma\varepsilon_{xf-ri}A_{xf-ri}(T_{xf,surf}^4-T_{bf}^4) + h_{xf-ri}A_{xf-ri}(T_{xf,surf}-T_{ri}) + \dot{m}_{evap}hg_{xf,surf}$$

xf-ri (35)

The riser, downcomer and film temperature distributions are:

$$T_{xf,out} = T_{xf} \qquad T_{lf,in} = T_{lf} \qquad T_{lf,out} = T_{lf}$$

Films (36)

$$T_{dc} = \frac{T_{dc,in}+T_{dc,out}}{2} \qquad T_{ri} = \frac{T_{ri,in}+T_{ri,out}}{2}$$

Air Paths (37)

REFERENCES

1. I. H. Shames, *Mechanics of Fluids*, McGraw-Hill Book Company, 1962.

2. A. H. Shapiro, *The Dynamics and Thermodynamics of Compressible Fluid Flow*, The Ronald Press Company, New York, 1953.

3. W. F. Hughes and J. A. Brighton, *Theory and Problems of Fluid Dynamics*, McGraw-Hill Book Company, 1967.

4. R. B. Bird, W. E. Stewart, and E. N. Lightfoot, *Transport Phenomena*, John Wiley & Sons, 1960.

5. NUREG/CR-5809 EGG-2659, "An Integrated Structure and Scaling Methodology for Severe Accident Technical Issue Resolution", INEL, EG&G Idaho, Inc.

APPENDIX B
DEVELOPMENT OF CONTAINMENT PRESSURIZATION EQUATION

DEVELOPMENT OF CONTAINMENT PRESSURIZATION EQUATION

The containment transient mass and energy equations include time derivatives of internal energy that confuse the relationship between the other terms in the equation. However, the mass and energy equations for the containment gas can be manipulated to produce a single equation that is more convenient for expressing the containment pressurization in terms of well defined terms. The single expression does not eliminate variables, so it is still necessary to evaluate the individual mass transport terms and the convective energy transport terms. A form of the combined mass and energy equations is first developed in terms of temperature, followed by the development of a form in terms of pressure and volumetric flow rates for the mass transport terms and temperatures for the convective heat transfer terms.

The containment gas volume is forced by the break steam source and interacts with the six structure groups, the pool, and the IRWST. The containment steam and air mass conservation equations can be written:

$$\frac{dm_{ct,stm}}{dt} = \dot{m}_{stm,in} - \sum_{i=1}^{6} \dot{m}_{ct-lf,i} + \dot{m}_{ct-pl} - \dot{m}_{ct-rw}$$

$$\text{and} \quad \frac{dm_{ct,air}}{dt} = 0 \tag{1}$$

and the energy equation:

$$\frac{d}{dt}(m\,ug)_{ct} = (\dot{m}\,hg)_{stm,in} - hg_{ct,stm}\sum_{i=1}^{6}\dot{m}_{ct-lf,i} + hg_{pl,stm}\dot{m}_{pl-ct} - hg_{ct,stm}\dot{m}_{ct-rw}$$

$$- \sum_{i=1}^{6} h_{lf,i}A_{ct-lf,i}(T_{ct}-T_{lf,surf,i}) + h_{pl}A_{ct-pl}(T_{pl,surf}-T_{ct}) - h_{rw}A_{ct-rw}(T_{ct}-T_{rw,surf}) \tag{2}$$

An equation of state for the gas is also required, in addition to Equations 1 and 2, to solve for containment pressure. The equation of state for an ideal gas is assumed and used in the following forms:

$$P = \rho R T \quad \text{or} \quad PV = mRT \quad \text{or} \quad hg - ug = \frac{P}{\rho} \tag{3}$$

The right side of the energy equation includes steam mass fluxes and convective heat transfer terms that eventually will require knowledge of the air/steam ratio to evaluate. The left side of the energy equation is a time derivative of the total internal energy. The total internal energy is the sum of the air and steam internal energies:

$$(mug)_\alpha = (mug)_{\alpha,stm} + (mug)_{\alpha,air} \qquad (4)$$

a,c

Substituting the mass equation into Equation 6, replacing the left side of Equation 2 with the result, and combining terms gives a combined mass and energy equation:

a,c

The definition of enthalpy for a perfect gas, $hg = ug + RT$, can be used to write:

$$\begin{aligned} hg_2 - ug_1 &= ug_2 + RT_2 - ug_1 \\ &= c_v(T_2 - T_1) + RT_2 \end{aligned} \qquad (8)$$

Substituting Equation 8 into Equation 7 produces a combined mass-energy equation in terms of temperature:

$$\begin{bmatrix} \end{bmatrix} \quad a,c$$

With appropriate substitutions, Equation 9 can be expressed in terms of pressure. Taking the total derivative of the equation of state, $T = PV/mR$ gives:

$$\begin{bmatrix} \end{bmatrix} \quad a,c$$

Note that $c_v T$ is not equal to ug, and that temperatures are absolute. With the substitutions $R = c_p - c_v$ and $\gamma = c_p/c_v$ Equation 10 can be expressed as:

$$\begin{bmatrix} \end{bmatrix} \quad a,c$$

Writing Equation 11 for air and for steam, and adding the two equations gives:

$$\begin{bmatrix} \end{bmatrix} \quad a,c$$

With $P = P_{air} + P_{stm}$, $dm_{air}/dt = 0$, and differentiating PV, Equation 12 can be written:

$$\begin{bmatrix} \end{bmatrix} \quad a,c$$

Equation 13 can be combined with Equations 1 and 9 to give:

$$\left[\right]^{a,c} \tag{14}$$

With the substitution $\rho C_p T = \gamma P/(\gamma-1)$ Equation 14 can be written in terms of pressure and volumetric flow rate as:

$$\left[\right]^{a,c} \tag{15}$$

The expression for dV/dt will normally be zero, unless it is desired to calculate the small value of containment pressurization due to displacement of containment volume by water.

Equations 9, 14, and 15 are different forms of the same equation that combine the energy conservation, mass conservation and state equations into single expressions for pressure inside containment.

APPENDIX C
PARAMETRIC CALCULATION OF STEADY-STATE HEAT AND MASS TRANSFER
FROM CONTAINMENT TO EXTERNAL ENVIRONMENT

PARAMETRIC CALCULATION OF STEADY-STATE HEAT AND MASS TRANSFER FROM CONTAINMENT TO EXTERNAL ENVIRONMENT

The equations governing heat and mass transfer from the inside of containment to the external film can be solved directly, given known internal conditions of temperature and pressure, for an assumed external film temperature. Similarly, the equations governing heat and mass transfer from the external film temperature can be solved if the other external conditions are known. These other external conditions can be assumed, the temperature and fluxes calculated and used to validate the assumed conditions. With some insight from tests and other calculations, this process has been found to be very efficient, using the external film temperature as a parameter. The process is applicable to both the AP600 and the large-scale tests. Figure C-1 shows the parametric solution for a large-scale test for internal conditions of approximately 230°F and 33 psia. Application of the parametric solution to AP600 is similar. The solutions for condensation, evaporation, and external conditions are developed in the following sections, with examples.

Condensation

The condensation rate is given as a function of the containment heat pressure and temperature:

$$\dot{m}'' = K_g M (P_{cont} - P_{surf}) \tag{1}$$

where P_{cont} is partial pressure of steam in containment
P_{surf} is partial pressure of steam at the film surface
M is the molecular weight of steam
and K_g is the mass transfer coefficient given by:

$$K_g = 2.75E-4(T_{avg})^{0.81} \frac{h}{k P_{bm} M}, \qquad [\frac{lbm}{hr-ft}] \tag{2}$$

where k is the steam thermal conductivity
T_{avg} is the average temperature between the containment and the surface in degrees R
P_{bm} is the log-mean pressure difference between the air partial pressure in containment and the air partial pressure at the surface
and h is the free convection heat transfer coefficient given by:

$$h = 0.13k \left(Pr \frac{\rho_{surf} - \rho_{cont}}{\rho_{avg} v^2 g} \right)^{\frac{1}{3}} \tag{3}$$

where Pr   is the Prandtl Number

ρ_{surf} is the total density (steam+air) at the film surface

ρ_{cont} is the total density (steam+air) in containment

v is the kinematic viscosity

and ρ_{avg} is the average density between the film surface and containment

The total heat transferred into the shell under steady state conditions is a combination of free convection, condensation, and film flow downward along the interior wall.

$$q''_{shell} = h(T_{cont} - T_{surf}) + \dot{m}'' h_g - \dot{m}'' h_f \tag{4}$$

where h_g is the enthalpy of saturated steam at the partial pressure of steam at the film surface

h_f is the saturated liquid enthalpy at the film surface temperature

T_{cont} is the containment temperature

and T_{surf} is the film surface temperature

Finally, the temperature drop through the internal film, coated steel vessel wall, and the external film is calculated by:

$$T_{xf-surf} = T_{if-surf} - \frac{q''_{shell}}{\left(\dfrac{2\delta_{film}}{k_{film}} + \dfrac{\delta_{steel}}{k_{steel}} + \dfrac{2\delta_{coating}}{k_{coating}} \right)^{-1}} \tag{5}$$

where the first term in the denominator represents the thermal resistance of the two liquid films, the second term represents the thermal resistance of the steel shell, and the third term represents the thermal resistance of the inside and outside coatings.

Equation 5 relates the external film surface temperature to the internal conditions. A similar relationship can be developed using the equations that govern evaporation off the external film to relate the external film surface temperature to the external conditions.

Evaporation

The equations governing evaporation from the external film are substantially the same as those governing condensation on the internal film.

The evaporation rate is given as a function of the external annulus pressure and temperature:

$$\dot{m}'' = K_g M (P_{ann} - P_{surf}) \tag{6}$$

where P_{ann} is partial pressure of steam in the annulus

P_{surf} is partial pressure of steam at the film surface

M   is the molecular weight of the steam

and K_g is the mass transfer coefficient given by:

$$K_g = 2.75 \times 10^{-4} T_{avg}^{0.81} \frac{h}{k P_{bm} M} \tag{7}$$

where   k   is the steam thermal conductivity

T_{avg} is the average temperature between the annulus and the film surface

P_{bm} is the log-mean pressure difference between air partial pressure in the annulus and the air partial pressure at the film surface

and   h   is the forced convection heat transfer coefficient given by:

$$h = 0.023 \frac{k}{d} Pr^{1/3} \left(\frac{vd}{\nu}\right)^{0.8} \tag{8}$$

where   Pr   is the Prandtl Number

d   is the hydraulic diameter of the annulus

v   is the air velocity in the annulus

and ν is the kinematic viscosity

The total heat transferred from the shell into the annulus air under steady state conditions is a combination of forced convection, evaporation, and enthalpy transported downward by the film flow. The air velocity in Equation 8 is an important parameter. However, air velocities are known, or specified for the large scale tests. For AP600, the air velocity is estimated, treated as a known value, and subsequently validated and adjusted if necessary with the calculated results.

$$\dot{q}''_{shell} = h(T_{surf} - T_{ann}) + \dot{m}'' h_g - \dot{m}'' h_f \tag{9}$$

where h_g is the enthalpy of saturated steam at the partial pressure of steam at the film surface

h_f is the saturated liquid enthalpy at the film surface temperature

T_{ann} is the annulus temperature

and T_{surf} is the film surface temperature

Equation 9 relates the external film surface temperature to the heat transfer form the shell to the external film using the evaporation equations. For steady-state, the shell heat flux as calculated using the condensation equations (Eqs. 1-5), must match the shell heat flux as calculated using the evaporation equations (Eqs. 6-9). The solution can be matched to the measured LST test results to determine the validity of the method.

Large-Scale Test Comparison

For the purpose of validating this method of determining the external heat transfer, a steady-state test was chosen, which is similar to expected internal containment conditions for AP600 2000 seconds into a design basis LOCA. The key parameters of this test are summarized in Table C-1.

Four separate heat transfer regions exist on the exterior of the test vessel:

1. A dry region, where very little heat transfer occurs

2. A subcooled wet region where the temperature of the liquid film is increased from the temperature at application to the saturated temperature. Over this region, little evaporation occurs. It is also likely that the internal steam-to-air ratio is slightly steam-rich, due to the tendency of the steam plume to rise to the top of the vessel.

3. A saturated wet region where the temperature remains constant and the majority of the evaporation occurs.

4. The lower head which loses heat to the environment through free convection and radiation.

The dry area is given as a function of the water coverage and the surface heat transfer area:

$$A_{dry} = (1-frac)A_{tot}$$

For 92 percent coverage, $A_{dry} = 62.4 \text{ ft}^2$

To determine the area covered by subcooled water, the external film temperature must be determined where the external evaporative heat transfer is equal to the internal condensation heat transfer. This is accomplished by solving Equations 1 through 9 and plotting the condensation and evaporation heat transfer as a function of external film temperature. The external film temperature is the value where the two curves cross, as shown in Figure C-1. The temperature defined by this point is the saturation temperature where bulk evaporation occurs. For temperatures lower than this temperature, the heat transferred through the shell is assumed not to evaporate fluid, but rather to raise the sensible heat of the film from the application temperature to the saturation temperature. This region is defined as the subcooled region.

For this case:

$$T_{sat} = 158°F \quad \text{and}$$

$$\dot{q}''_{shell-saturated} = 1.267 \frac{Btu}{sec-°F}$$

The total heat transferred to the film to raise its temperature to 158°F is given by:

$$\dot{q}_{subcooled} = \dot{m}_{xf} C_p (T_{sat} - T_{xf-applied})$$

For this case,

$$\dot{q}_{subcooled} = 180.64 \ BTU/sec$$

The average external film surface temperature in the subcooled region is given by:

$$\bar{T}_{xf-surf} = \frac{T_{xf-applied} + T_{sat}}{2}$$

The heat flux in the subcooled region can be calculated with the condensation model (Eqs. 1-5) and this external film temperature. To correctly calculate the condensation heat transfer, it is important to specify the internal steam and air partial pressures correctly. Using the condensation model with the correct steam and air pressure gives a heat flux in the subcooled region of 1.916 Btu/sec-ft².

Thus the shell surface area covered by the subcooled film is:

$$A_{subcooled} = \frac{\dot{q}_{subcooled}}{\dot{q}''_{shell}} = 94.28 \ ft^2$$

and the area covered by the saturated film is:

$$A_{saturated} = A_{tot} - A_{dry} - A_{subcooled} = 622.9 \ ft^2$$

The heat transferred by the dry area is given by:

$$\dot{q}_{dry} = A_{dry}[h(T_{surf} - T_{annulus}) + \sigma\varepsilon(T_{surf}^4 - T_{baffle}^4)]$$

For this case,

$$\dot{q}_{dry} = 4.93 \text{ BTU/sec}$$

And the heat transferred through the bottom head is given by:

$$\dot{q}_{bottomhead} = A_{bottomhead}[h(T_{surf} - T_{ambient}) + \sigma\varepsilon(T_{surf}^4 - T_{ambient}^4)]$$

For this case,

$$\dot{q}_{bottom\ head} = 7.26 \text{ Btu/sec}$$

A heat balance on the shell can be used to check the model against the measured test results.

$$\dot{q}_{tot} = \dot{q}_{subcooled} + \dot{q}''_{shell-sat}A_{sat} + \dot{q}_{dry} + \dot{q}_{bottomhead} = 629 \text{ BTU/sec}$$

The total heat lost from the steam is given by:

$$\dot{q}_{tot} = \dot{m}_{steam}h_{g-steam} - \sum \dot{m}_{condensate}h_{f-condensate} = 629 \text{ BTU/sec}$$

Although perfect agreement between measured and predicted energy balances are fortuitous, the heat transfer from the inside of the containment shell to the environment is accurately predicted by the condensation and evaporation models described above. The results of this analysis can be used to define Pi-groups to compare with the AP600 containment, and determine the applicability of the test results to the prototype.

Pi-Groups

Pi-groups representing components of external heat transfer were developed to determine the applicability of the large-scale test results to the AP600. These Pi-groups are ratios of the individual

heat transfer components to the heat input to the vessel from the steam flow. The Pi-groups for Test 222.1 are summarized in Table C-2.
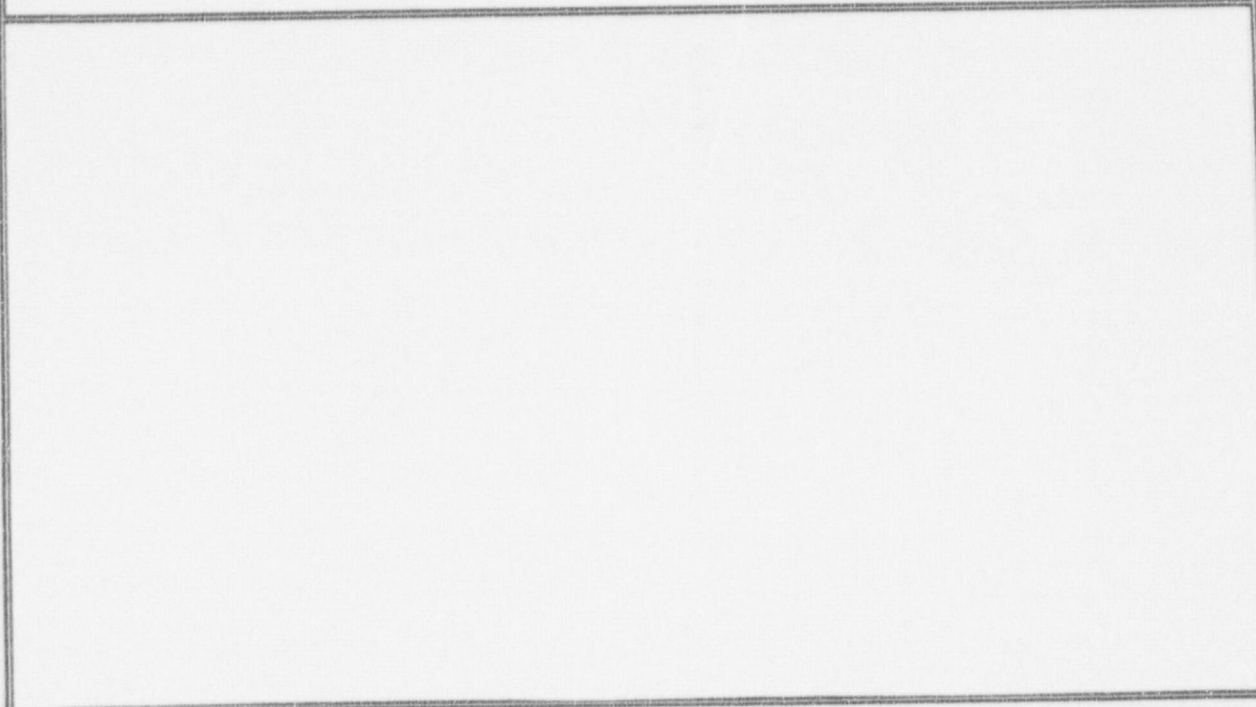
Conclusions

Based on these calculations, the equations governing condensation and evaporation accurately predict the large-scale test results.

TABLE C-1
LARGE-SCALE TEST NO. 222.1, KEY PARAMETERS

a,c

TABLE C-2
LST 222.1 HEAT FLUXES AND PI-GROUPS

a,b

Figure C-1 Evaporation and Condensation vs. External Film Surface Temperature
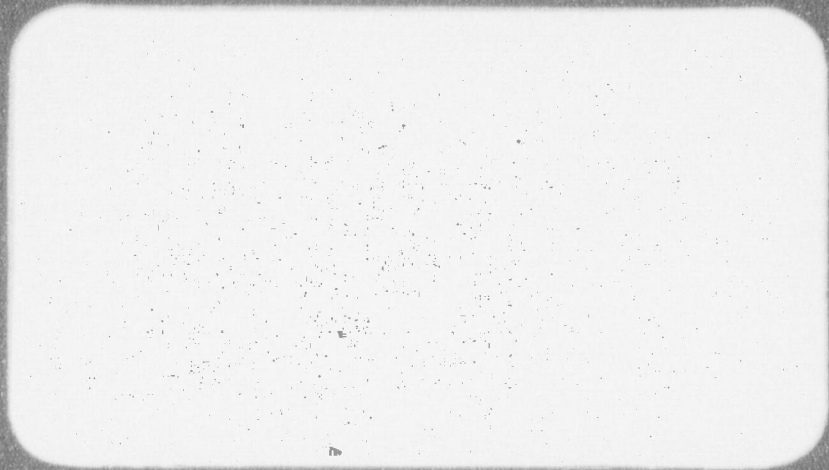
Westinghouse Energy Systems

Westinghouse Energy Systems

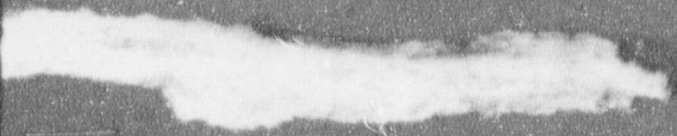Westinghouse Energy Systems